2014

Multimaterial fibers in photonics and nanotechnology

Guangming Tao
University of Central Florida

MULTIMATERIAL FIBERS IN PHOTONICS AND NANOTECHNOLOGY

by

GUANGMING TAO
B.S. Shandong University, China, 2006
M.S. Fudan University, China, 2009
M. S. University of Central Florida, USA, 2012

A dissertation submitted in partial fulfillment of the requirements
for the degree of Doctor of Philosophy
in CREOL, The College of Optics & Photonics
at the University of Central Florida
Orlando, Florida

Spring Term
2014

Major Professor: Ayman F. Abouraddy

ABSTRACT

Recent progress in combing multiple materials with distinct optical, electronic, and thermomechanical properties monolithically in a kilometer-long fiber drawn from a preform offers unique multifunctionality at a low cost. A wide range of unique in-fiber devices have been developed in fiber form-factor using this strategy. Here, I summary my recent results in this nascent field of 'multimaterial fibers'. I will focus on my achievements in producing robust infrared optical fibers and in appropriating optical fiber production technology for applications in nanofabrication.

The development of optical components suitable for the infrared (IR) is crucial for applications in this spectral range to reach the maturity level of their counterparts in the visible and near-infrared spectral regimes. A critical class of optical components that has yet to be fully developed is that of IR optical fibers. Here I will present several unique approaches that may result in low-cost, robust IR fibers that transmit light from 1.5 microns to 15 microns drawn from multimaterial preforms. These preforms are prepared exploiting the newly developed procedure of multimaterial coextrusion, which provides unprecedented flexibility in material choices and structure engineering in the extruded preform. I will present several different 'generations' of multimaterial extrusion that enable access to a variety of IR fibers. Examples of the IR fibers realized using this methodology include single mode IR fibers, large index-contrast IR fibers, IR imaging fiber bundles, IR photonic crystal and potentially photonic band-gap fibers.

The complex structures produced in multimaterial fibers may also be used in the fabrication of micro- and nano-scale spherical particles by exploiting a recently discovered in-fiber Plateau-Rayleigh capillary instability. Such multimaterial structured particles have promising application

in drug delivery, optical sensors, and nanobiotechnology. The benefits accrued from the multimaterial fiber methodology allow for the scalable fabrication of micro- and nano-scale particles having complex internal architectures, such as multi-shell particles, Janus-particles, and particles with combined control over the radial and azimuthal structure.

Finally, I will summarize my views on the compatibility of a wide range of amorphous and crystalline materials with the traditional thermal fiber drawing process and with the more recent multimaterial fiber strategy.

To my parents.

ACKNOWLEDGMENTS

First of all, I would like to express my appreciation to my PhD advisor Prof. Ayman F. Abouraddy for guiding me and supporting me over these years. Thank him for being such great role models for me and teaching me in both academic and life skills.

I also want to thank my doctoral dissertation committee members Prof. Guifang Li, Prof. Leonid Glebov, and Prof. Robert Peale for their great support during my PhD study, and their valuable comments and suggestions throughout this work.

I want to thank all my colleagues, who generously share their thoughts and knowledge with me. It gave me a wonderful experience to work with these smart and nice guys. I got tremendous help and encouragement from many friends and scientists in both academia and industry in last few year during my study at CREOL/UCF, however, I would prefer not to simply list their name here but keep them in my heart.

Several year ago, someone told me that *the world is more nonlinear than we think*. I think I have much better understating about life now. Everything is changing. I appreciate everything in my life.

To someone who are interested in my research, please check APPENDIX Section for more details and update about my current research and future prospects.

This dissertation is dedicated to my beloved parents.

TABLE OF CONTENTS

LIST OF FIGURES

LIST OF TABLES

CHAPTER 1 INTRODUCTION OF MULTIMATERIAL FIBERS

1.1 Emergence of multimaterial fibers

Optical fibers have improved the quality of life throughout the world and have fundamentally altered the human condition in both obvious and imperceptible ways. The internet, and most telecommunications, is delivered across the globe today through optical fibers [1] [2]. In addition, optical fibers are used in a multitude of applications ranging from noninvasive medical surgery [3] [4] to structural-integrity monitoring of bridges and oil pipelines [5] [6], and fiber lasers are finding applications in materials processing and manufacturing [7]. One of the most striking features of these advances is that optical fibers are remarkably simple devices from the perspective of materials composition. The majority of optical fibers in use today are fabricated from a single material: silica glass. While optical fibers made of other glasses or polymers have also been developed, silica glass remains the dominant material in producing optical fibers.

The mid 1990's witnessed the development of new classes of optical fibers, photonic crystal fibers (PCF's) and photonic band gap fibers [8], founded in new optical physics initiated with the concept of photonic band gaps (PBG's) [9]. Unexpectedly, these advances were also eye-opening with regards to the perceived limitations of the structures that may be produced by the traditional process of thermal fiber drawing. In fact, the initial proposal for fabricating silica PBG fibers was dismissed as unfeasible by seasoned practitioners [10] even though no new material was combined with silica, only air holes. Nevertheless, the rapid success of PBG fibers has had unexpected consequences for the process of fiber fabrication itself. One such consequence was the introduction of the concept of 'multimaterial fibers' over the past decade. This new class of fibers

leverages the capabilities of traditional fiber fabrication, but aims at developing new fiber structures, functionalities, and applications that stem from altering the materials composition of the fiber. It is difficult to provide a conclusive and all-encompassing definition of this nascent concept. For the first time, we define multimaterial fibers to be *high-aspect-ratio structures that comprise multiple distinct materials, typically produced by thermal drawing from a macroscopic scaled-up model called a 'preform'*. Materials with different optical, electronic, thermo-mechanical, and acoustic properties have now been incorporated into the fiber form-factor [11]. The set of fabrication approaches developed in this emerging field are introducing new functionalities that are not usually associated with optical fibers. Examples include fibers that produce an electrical signal when light is incident on the fiber external surface [12] [13] [14] or when the temperature of the ambient environment changes [15]; fibers that monitor their own performance and structural integrity [16]; flexible, lightweight fiber arrays that image the surrounding environment [14] [17]; and fibers that produce or detect sound or ultrasonic signals [18] [19]. Fiber drawing is therefore morphing into a fabrication route for producing electronic and optoelectronic fiber devices that may also be potentially incorporated or woven into fabrics, thereby endowing them with new and sophisticated functionalities [11].

New ways of thinking of the fiber drawing process itself are now emerging with the advent of multimaterial fibers. Through dimensional reduction, nanostructures such as nanowires with few-nanometer diameters and unprecedented lengths may be produced [20] [21] [22] [23]. The fiber cladding may be viewed as a crucible for chemical synthesis with the reactive agents placed in the core [24]. Multimaterial fibers are also a new playground for the controllable study of fluid dynamics in confined space and over a wide range of scales [25]. These developments have

recently led to a scalable, top-down, in-fiber fabrication process capable of producing complex structured particles over an unprecedented range of diameters spanning both micro- and nano-scales [26].

There are two aspects of fiber production that have been appropriated by the emerging field of multimaterial fibers. First, the process typically starts by preparing a macroscopic preform. Since the preform diameter is on the centimeter scale, it is straightforward to create a complex transverse cross section with controllable placement of structures incorporating multiple materials. Second, thermal fiber drawing is inherently scalable, producing kilometers of fiber with accurate control over size and axial uniformity [27]. In order for the fiber to maintain the complex transverse structure of the multimaterial preform, restrictions are placed on the allowable materials combinations compatible with this fabrication process. There are some exceptions to this overall approach. For example, multimaterial fibers may be produced starting with a single-material fiber or wire used as a scaffold for additive manufacturing, such as dip coating on the outer surface of extended fiber lengths [28] or vapor deposition inside hollow enclaves in short lengths of a pre-existing fiber [29].

1.2 Material constraints and fiber drawing

Optical fibers are typically drawn thermally from a macroscopic preform in a fiber draw tower, such as that shown schematically in Fig. 1.1(a), known as the preform-to-fiber approach [30]. The preform is fed into a furnace that softens the material, after which gravity or an external force ‘pulls’ the molten gob at the preform tip until it stretches into a thin strand whose diameter

is monitored with a gauge. Figure 1.1(b) is the photograph of fiber tower at CREOL, The College of Optics & Photonics, University of Central Florida for multimaterial fiber drawing. If necessary, polymer coatings are added to the fiber surface for mechanical protection. This relatively simple fabrication process is behind the thousands of kilometers of optical fiber used in the communications networks that span the globe today [1][2]. Alternatively, the double-crucible method [31] has been used to produce optical fibers from glass melts of the core and cladding that are pushed through a nozzle. There have been no reports to date on multimaterial fibers produced by this method.

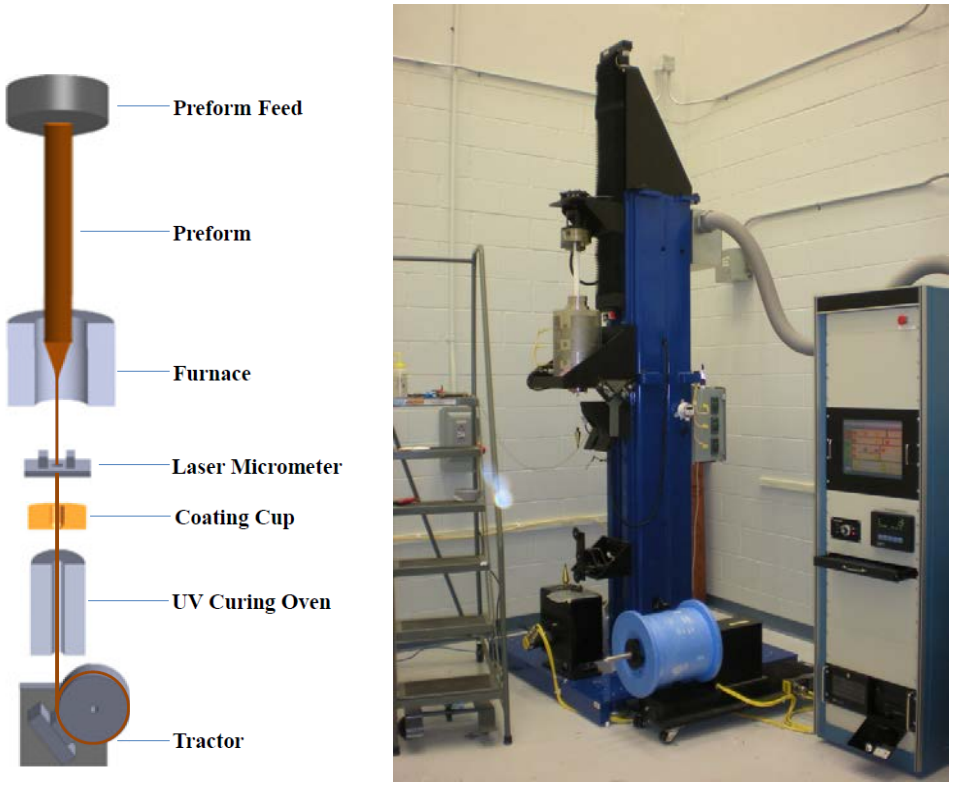

(a) (b)

Figure 1.1 (a) Schematic of the thermal fiber drawing process in a draw tower. (b) Photograph of fiber tower at CREOL, UCF

When the preform consists of a single material, the viscosity at the drawing temperature dictates the parameters of the draw, such as the drawing speed. Multimaterial preforms, on the other hand, may contain materials that are incompatible with thermal drawing when each taken separately, such as crystalline semiconductors or metals. Using the thermal drawing process, therefore, imposes constraints on the materials combinations that are compatible with this fabrication approach. In order to gain insight into the feasibility of various materials combinations, we present in Fig. 1.2(a) the viscosity of silica glass, silicon, and gold as a function of temperature. These materials are chosen to represent three distinct materials classes from the electronic perspective: an amorphous insulator, a crystalline semiconductor, and a metal, respectively, in addition to their different optical and mechanical properties. The softening temperature of silica ranges from 1400 to 2350 °C, thereby offering a broad range of drawing conditions. Silicon and gold, on the other hand, are characterized by an abrupt drop in their viscosities above their melting temperature T_m, where a phase transition takes place. Nevertheless, silica may be used as a 'cladding' in which a silicon or gold 'core' is embedded with the preform thermally drawn above the core T_m. In this scenario, the cladding acts as a scaffold to contain and restrict the flow of the low-viscosity core material.

From this example we may outline the general constraints on the construction of multimaterial preforms and the drawing conditions. At least one material should be amorphous, typically a glass or polymer, and resist devitrification during thermal drawing. This 'backbone' material forms an outer cladding that supports the other materials during the draw and maintains the cross-sectional structure of the fiber. The amorphous material constituents must be chosen to have overlapping softening temperatures, while the crystalline constituents must have T_m below

the drawing temperature. The drawing temperature must be lower than the boiling temperature of the core material. Additionally, care must be taken to avoid fluid instabilities that may occur when the viscosity of the materials is lowered and the transverse dimensions reduced. The materials must also have relatively similar thermal expansion coefficients in the temperature range extending to the drawing temperature in order to avoid mechanical fractures resulting from thermo-mechanical mismatches.

In Fig. 1.2(b) we present the viscosity of a wide range of *amorphous* materials. Some glasses (such as soda-lime-silica) have a broad temperature range suitable for thermal drawing, while others (such as fluorides, chalcogenides, and tellurites) have a relatively narrower temperature window. In Fig. 1.2(c) we plot the viscosity of some typical *crystalline* materials above their T_m. Using Fig. 1.2(b) and Fig. 1.2(c) together, it is possible to choose potential pairs of amorphous-crystalline materials that may be combined in a preform and co-drawn into a multimaterial fiber. For example, it is possible to draw Si, Ge, or gold clad with silica glass; InSb clad with soda-lime-silica glass glass; or Sn or Se clad with fluoride or chalcogenide glass, or even a polymer. For completeness, we identify in Fig. 1.2(d) the glass transition temperature T_g of the amorphous materials and the melting temperature T_m of crystalline materials used in Fig. 1.2(a)-(c) versus the linear thermal expansion coefficient (TEC). While there are other critical aspects that must be considered in the materials selection to successfully draw a multimaterial fiber, Fig. 1.2 offers the basic groundwork for the potential materials pairings. Finally, we note that more than two materials chosen according to the above criteria may be incorporated in the same multimaterial fiber. This feature enables the construction of in-fiber electronic and optoelectronic devices.

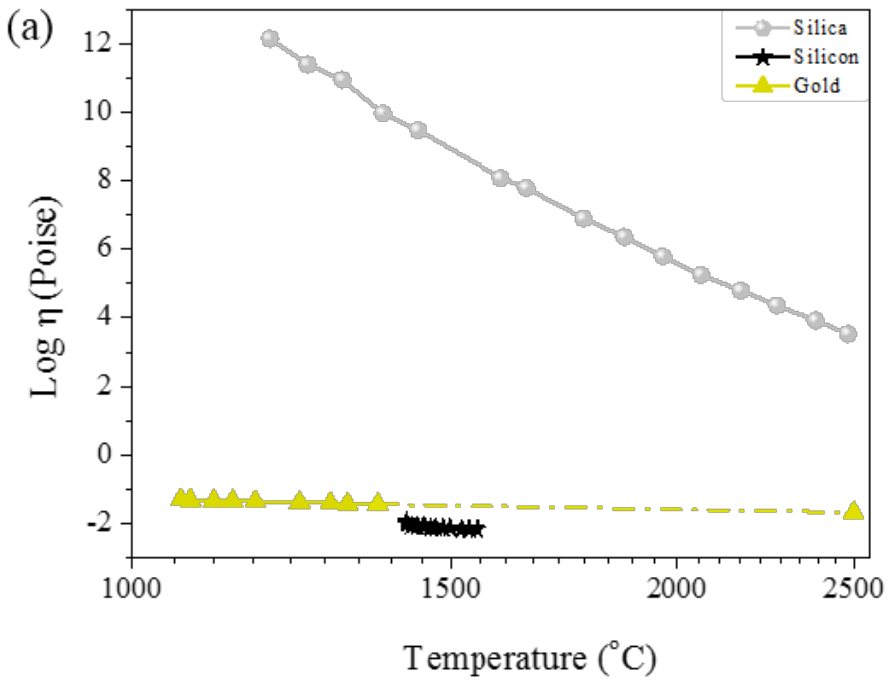
(a)
Silica
Silicon
Gold
Log η (Poise)
Temperature (°C)
12
10
8
6
4
2
0
-2
1000
1500
2000
2500

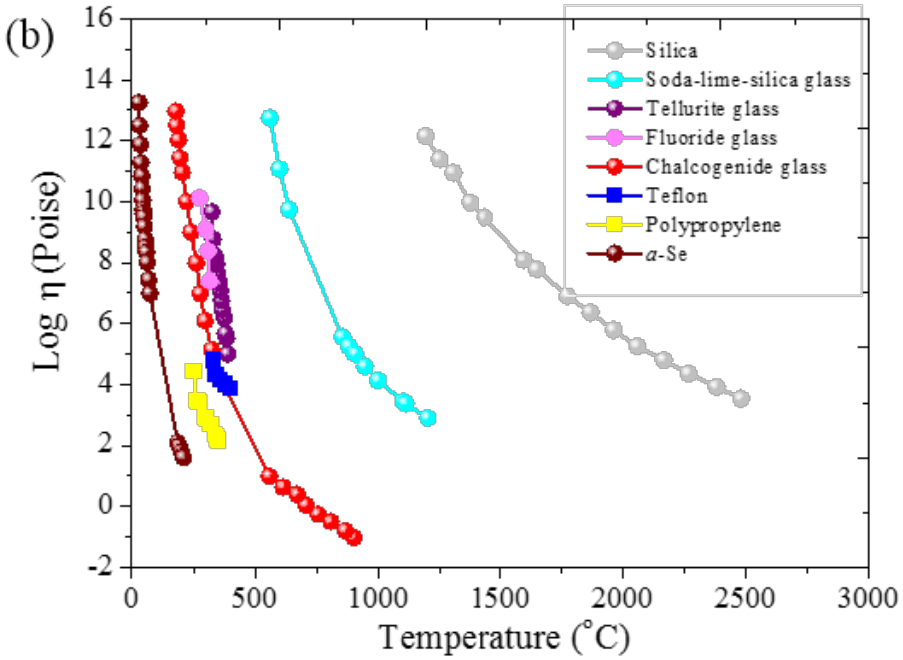
(b)
Silica
Soda-lime-silica glass
Tellurite glass
Fluoride glass
Chalcogenide glass
Teflon
Polypropylene
α-Se
Log η (Poise)
Temperature (°C)
16
14
12
10
8
6
4
2
0
-2
0
500
1000
1500
2000
2500
3000

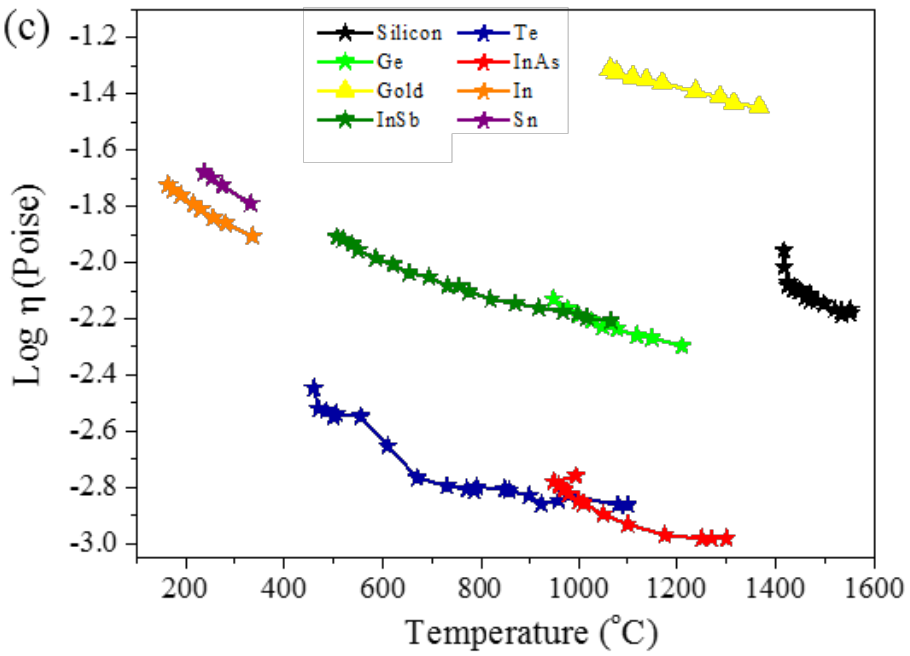
(c)
Silicon
Te
Ge
InAs
Gold
In
InSb
Sn
Log η (Poise)
-1.2
-1.4
-1.6
-1.8
-2.0
-2.2
-2.4
-2.6
-2.8
-3.0
200
400
600
800
1000
1200
1400
1600
Temperature (°C)

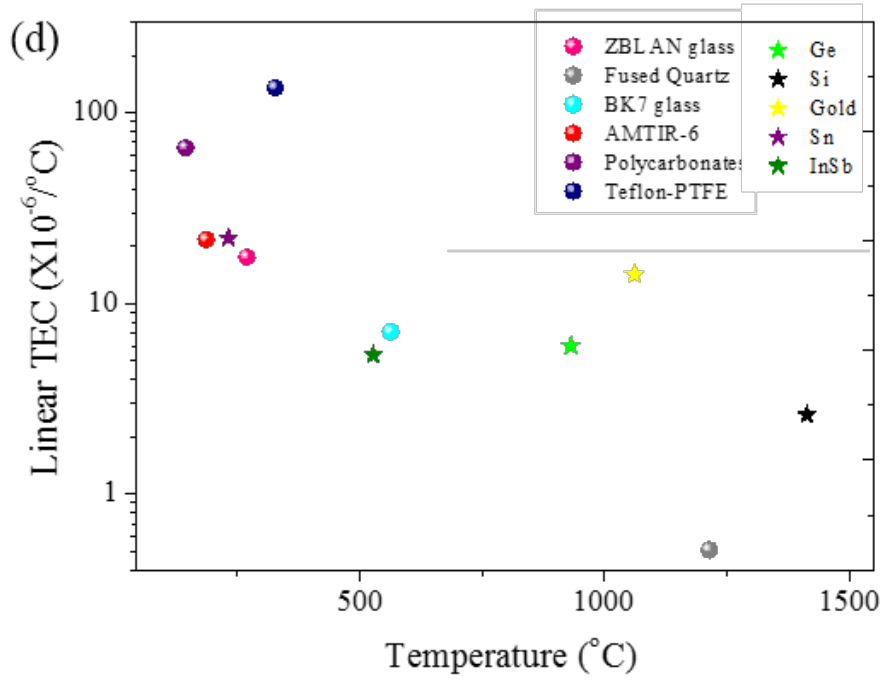
(d)
ZBLAN glass
Fused Quartz
BK7 glass
AMTIR-6
Polycarbonates
Teflon-PTFE
Ge
Si
Gold
Sn
InSb
Linear TEC (X10-6/°C)
100
10
1
500
1000
1500
Temperature (°C)

Figure 1.2 Dynamic viscosity (logarithm of viscosity g in poise) of selected materials versus temperature. (a) Viscosity for silica [32] silicon [33] and gold [34]. The viscosity for silicon and gold are measured above their melting temperatures. (b) Same as (a), showing the viscosity for silica [32], soda-lime-silica glass [35], fluoride glass[36], tellurite glass[37], chalcogenide glass (As_2S_3) [38], Teflon® PTFE-6 polymer[39], polypropylene (PP) polymer[40], and amorphous selenium[41]. (c) Same as (a), showing the viscosity for silicon[33], germanium[42], indium antimonide[43], tellurium[42], indium arsenide[42], indium[44], tin[44], and gold[34]. (d) Linear thermal expansion coefficient (TEC) at room temperature for selected materials plotted against the melting temperature (T_m) for metals and semiconductors (solid stars) and the glass transition temperature (T_g) for the amorphous materials (solid dots). References: Ge: T_m[45], TEC[46]; Si: T_m [45], TEC[47]; Gold: T_m [48], TEC[47]; Sn: T_m [48], TEC[49]; InSb: T_m [50], TEC[51]; Teflon® PTFE: T_g [52]; TEC[53]; Fused quartz: T_g [53], TEC[54]; BK7 glass: T_g [53], TEC[53]; AMTIR-6: T_g [55], TEC[55]; Polycarbonates: T_g [56], TEC[54]; ZBLAN glass: T_g [53], TEC[54].

1.3 Fiber preform fabrication

Four general classes of approaches to multimaterial preform preparation have been exploited thus far: (a) the rod-in-tube approach [57] [58] [59], (b) extrusion [60] [61] [62], (c) the stack-and-draw approach [8] [63], and (d) thin-film-rolling technology [11]. The choice is dictated by the materials used and the transverse structure targeted.

1.3.1 Rod-in-tube approach

Figure 1.3(a) depicts the rod-in-tube approach, which relies on inserting a rod of one material into a tube of another material to form a preform with a core-cladding structure. Alternatively, a powder may be placed in the tube and the preform sealed, which enables a wide range of materials to be incorporated into the core. If T_m of the core rod/powder is lower than the

drawing temperature, we designate the process molten-core-in-tube method. The recognition of the usefulness of this method for multimaterial fibers may be traced back to the pioneering work of E. Snitzer in 1989 [64], where selective volatization combined with the rod-in-tube method was used to produce a silica-clad fiber containing a soft-glass core. In this work, the drawing temperature was higher than T_m of a soft-glass core, and the high vapor pressure led to the volatilization of some compounds from the core, leaving a glass core with a different residual composition.

1.3.2 Extrusion

Extrusion is a process used to create objects with fixed cross-sectional profile by pushing a soft material through a die under pressure. J. Bramah patented the first extrusion process for producing lead pipes in 1797 [65], and E. Roeder [66] [67] [68] extended this approach to soda-lime silica, lead silicate, calcium aluminate and boric oxide glass in the 1970's. Material in the form of a rod, typically called a *billet*, is placed inside a sleeve held in a furnace (a vertically stacked billet is shown in Fig. 1.3(b) for demonstration). The billet is heated to the softening temperature of the incorporated materials and pressure is applied to push the material through a die that imparts shape to the extruded preform rod, which is subsequently drawn into a fiber. Using a multimaterial billet consisting, for example, of vertically stacked discs, the transverse structure of the extruded rod may be engineered [60] [62]. The two main advantages of this process over other manufacturing processes are its ability to create very complex cross-sections and work materials that are brittle, because the material only encounters compressive and shear stresses. Extrusion is also used to produce single-material complex MOF preform. D. Furniss and A. B. Seddon [5-27] had made some core/cladding glass preform by extrusion. K.M Kiang *et al.* [5-28]

reported the first MOF fabrication by extrusion. H. Ebendorff-Heidepriem *et al.* [5-29] reported a significant advance in preform extrusion and die design for the fabrication of complex structured preform using soft glass and polymer billets.

1.3.3 Stack-and-draw approach

The stack-and-draw approach has been used extensively in preparing the preforms drawn into microstructured fibers, PCFs, and PBG fibers [8]. The first demonstration of the stack-and-draw method to produce an optical fiber may be traced to Bell Labs in 1974 [73], at the dawn of the development of silica fibers, where a fiber containing a hanging core surrounded by air was produced. Rods, tubes, and/or plates from a single or multiple materials may be assembled into a preform [Fig. 1.3(c)] with dimensions determined by the targeted fiber structure. Multiple stack-and-draw steps may be applied recursively to reach the required dimensions and attain complex transverse structures. This approach is widely used for single-material MOFs [74]. However, Stacking is time-consuming and laborious, raises challenges for reproducibility, and is less suited to fragile soft glasses.

1.3.4 Thin-film rolling

Polymers may be incorporated into a fiber using any of the above three approaches. A unique process to incorporate a polymer in a preform is through rolling a thin polymer film followed by thermal consolidation under vacuum above the glass transition temperature of the constituent materials until the individual films fuse. An example of this process is shown schematically in Fig. 1.3(d), which details the fabrication approach towards making a multimaterial PBG fiber [75] [76] [77] [78] [79].

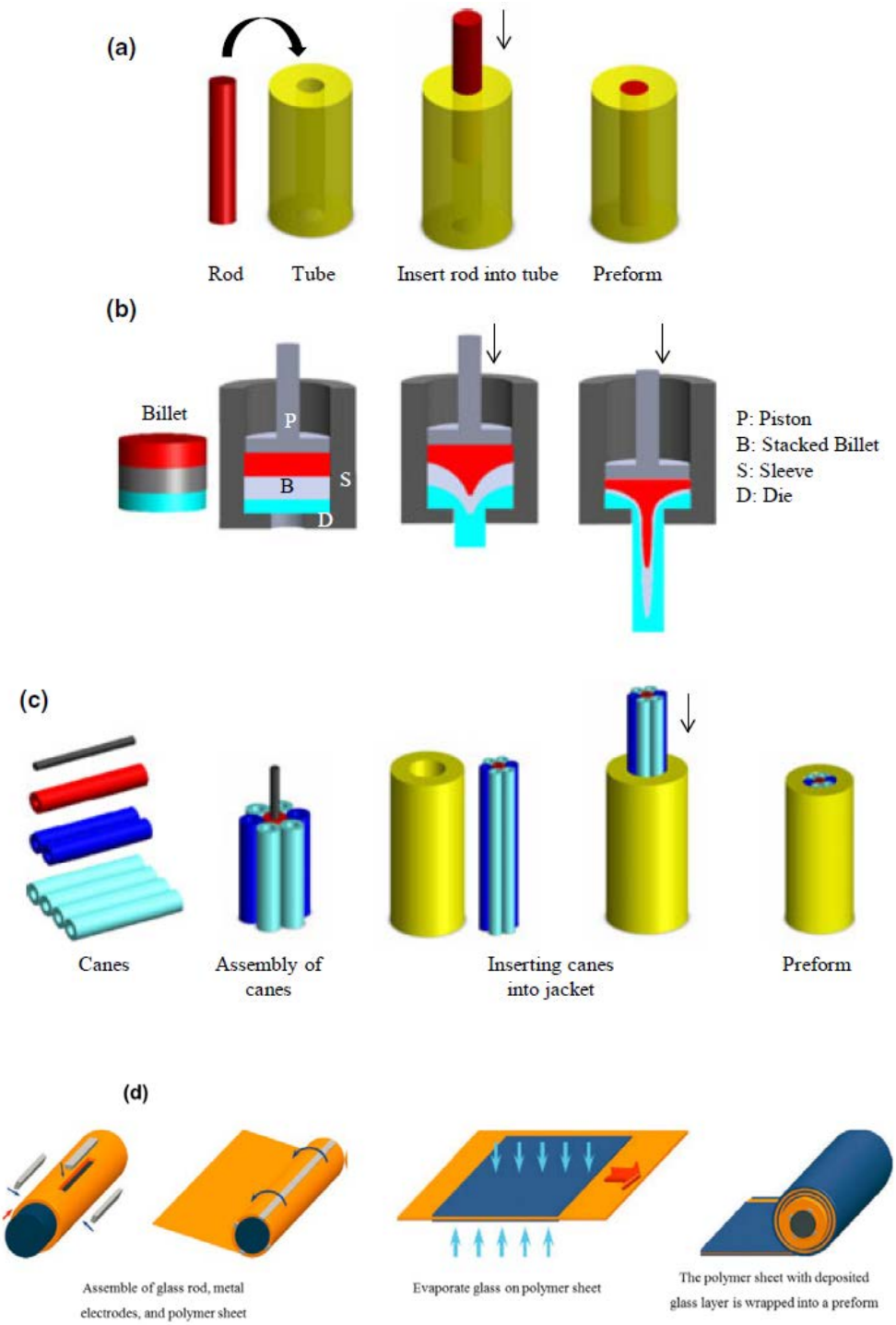

Figure 1.3 General methodologies for multimaterial fiber preform fabrication. (a) Rod-in-tube, (b) extrusion, (c) stack-and-draw methods, and (d) thin-film-rolling method. (Fig. 1.3.d is modified from [11])

The thin-film-rolling technique can also be performed recursively for realizing more complex cross-sections. For example, voids may be introduced into a post-consolidated structure. These voids may be filled by conductors and encapsulated in the preform by rolling additional thin films and reconsolidating. These multistep preform preparation processes form the basis for many photonic and optoelectronic multimaterial fiber devices [11] [80] [17] [81].

1.4 Other approaches for multimaterial fibers

We have described in the previous sections various multimaterial fibers that have been produced using the general methodology of preform-to-fiber fabrication. There are some interesting exceptions that we present briefly in this section. The first is an approach developed by Konarka, Inc., which starts from a long steel wire that is used in successive steps of dip-coating in organic solutions [28]. The result is a fiber with a multilayer coating along its whole length, forming an organic photovoltaic cell with ~ 3 % efficiency. The second approach uses a silica fiber with hollow enclaves (either a hollow-core fiber or a PCF) as a scaffold for vapor deposition of traditional crystalline semiconductors, a process typically called high-pressure microfluidic chemical deposition (HPMCD) [29] that extends the materials that may be incorporated into the fiber to single-crystal semiconductors [82] and polycrystalline elemental or compound semiconductors [83] [84]. High-pressure flow (2 – 1000 MPa) is used in silica microstructured optical fibers (MOF's) to overcome mass-transport constraints, resulting in uniform, dense, and conformal annular deposition onto hollow pore walls with uniformity on the order of 0.1 nm. Such an approach thus combines two well-developed fabrication methodologies, chemical vapor

deposition (CVD) [85] and silica fiber drawing. The basic idea is shown in Fig. 1.4(a), which involves heating small quantities of a high-pressure precursor within the interior of a MOF that decomposes upon heating to deposit on the walls in an amorphous state to ensure that it bonds smoothly, followed by annealing for crystallization. Figure 1.4(b) is an example of deposited doped semiconductor layers and metals [86]. As the annular deposited film grows thicker, the central holes from which depositions occurs becomes smaller until it is completely plugged and flow is extinguished. The empty pores in the MOFs are thus treated as micro- or nano-scale reaction chambers. A fiber-based device fabricated using this approach enabled all-optical modulation of 1.55-μm guided light via free-carrier absorption mediated by a 532-nm pump pulse [87]. Other examples include producing a ZnSe-core fiber [84], in-fiber Si and Ge wires and tubes used as field effect transistors [88], and in-fiber crystalline Si p–n homojunctions and Pt/n-type Si heterojunctions [86]. The HPCVD technique can accommodate different capillary core dimensions and may also be used to fill a large number of micro- and nano-scale pores in MOF's. The main drawback of this technology is the limited lengths of fiber devices produced compared to those resulting from fiber drawing.

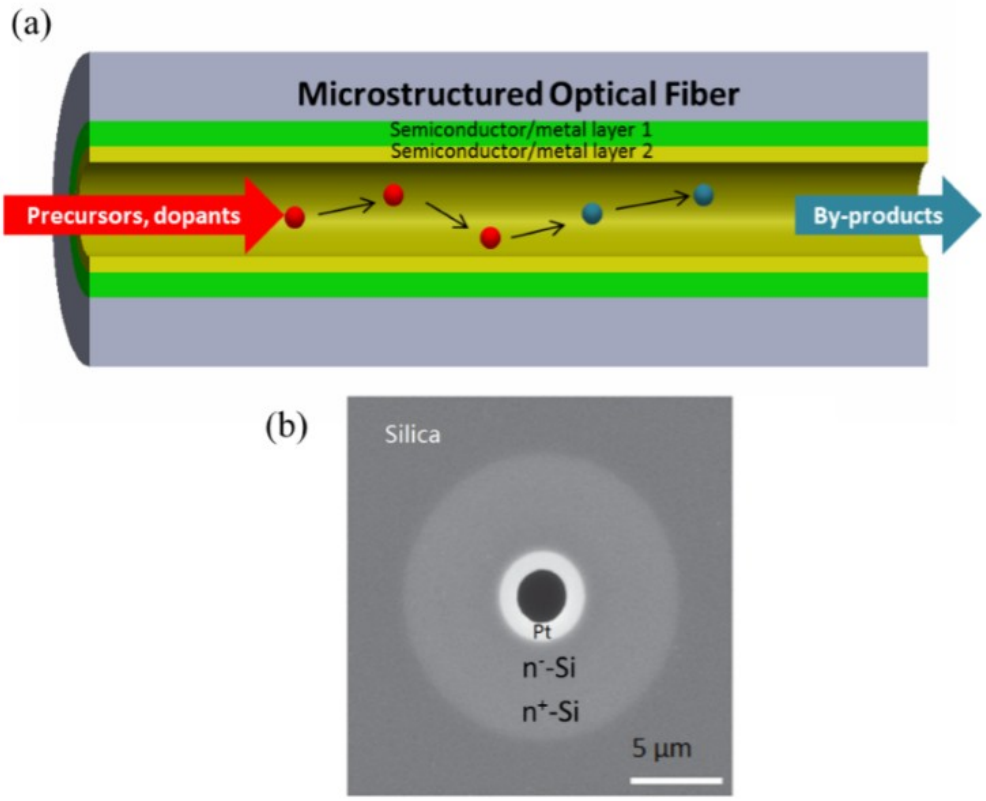

Figure 1.4 Integration of semiconductor junctions in MOFs. (a) Illustration of HPCVD in the MOF pores. (b) A Pt/n-Si Schottky junction formed by sequential deposition of phosphorous doped n+-Si, n--Si and platinum layers. [86].

CHAPTER 2 ROBUST MULTIMATERIAL CHALCOGENIDE GLASS INFRARED FIBERS

2.1 The importance of robust multimaterial infrared fibers

The development of quantum cascade lasers that span mid-infrared (MIR) wavelengths necessitate developing new infrared (IR) fibers capable of transmitting light in the MIR range. The main material candidates for producing IR fibers that cover this spectral region are polycrystalline silver halides and glassy chalcogenide glasses (ChGs). The latter are more chemically stable, and thus represent a superior choice for infrared fibers. The fabrication of robust infrared ChG fibers has long been hampered by the unfavorable mechanical characteristics typical of such glasses. Furthermore, the usual pathways to producing such fibers necessitate large-scale synthesis of high-purity glass, which represents a challenge in an academic environment, and thus presents an obstacle to the transfer of research results from academia to industry. In this chapter, I summary our progress on low-cost, robust MIR fibers with a broad transmission windows and low loss, which are thermally drawn from multimaterial preforms produced by several methodologies, including one-step multimaterial stacked coextrusion, high-efficiency multimaterial 'disc-to-fiber' coextrusion, and multimaterial 'rod-in-tube' coextrusion approaches. By combining our thin-film rolling technique, our robust IR fiber is thermally drawn in an ambient atmosphere into continuous lengths of fiber with desired core and diameters, desired core/cladding dimensional ratio and desired numerical apertures. These approaches offer alternative methodologies that overcome many of the traditional obstacles technology with reduced production cost.

Mid-wave and long-wave infrared or MIR wavelengths cover the important atmospheric windows of 3 – 5 μm and 8 – 12 μm, which hold important applications for the military, homeland security, and remote sensing. Furthermore, the MIR also covers the molecular fingerprints of numerous gases, liquids, and solids, which exhibit fundamental vibrational absorption bands with large extinction coefficients in the MIR (Figure 2.1). Recently, MIR sources (such as quantum cascade lasers, QCLs) have made possible real-time MIR spectroscopy [87]. However, there has not been a commensurate development of MIR delivery fibers, which limits the potential applications of such sources. To exploit the MIR spectral region effectively, it is essential to develop a host of accompanying MIR optical and photonic technologies, especially for MIR fibers. Optical fibers present a unique optical transmission modality that is particularly important for IR (non-visible), providing a mechanically flexible conduit that interfaces easily with other photonic devices.

In assessing the materials that are suitable for MIR transmission, we first consider the transparency range of common optical materials. Single crystals, such as silicon (Si), germanium (Ge), zinc selenide (ZnSe), and zinc sulfide (ZnS) are widely in infrared optical components. Polycrystalline halide material, such as AgBrCl, CsI, CdTe, BaF_2, GaAs, KBr, and KCl are also good candidates for MIR devices. Although several crystalline materials (whether single-crystal or polycrystalline) are transparent throughout this whole range, they present difficulties to fiber drawing, some lack chemical stability, typically have unfavorable mechanical characteristics, and cannot produce fibers with long lengths [88]. Nevertheless, both single-crystal and polycrystalline materials cannot be thermally drawn into a continuous fiber. This results from the abrupt phase transition above melting temperature, where these materials transition to a very low viscosity state

[89]. Non-glassy materials can also be drawn into fibers when provided with a glassy cladding. For example, germanium (Ge) was drawn into a fiber by J. Ballato et al. [57]. Nevertheless, such fibers typically do not demonstrate the same transmission window in their bulk counterparts due to irregularities along the fiber, micro-cracks which come from the mismatch of thermal expansion coefficients of the single-crystal core and the glassy cladding, and the last – but most important issue – is the current lack of available thermally compatible IR glassy materials that can serve as cladding. Recently developed silica-based microstructured hollow-core fibers may also become a candidate for IR beam delivery, but currently require a complex fabrication process and susceptibility to additional bending losses [90].

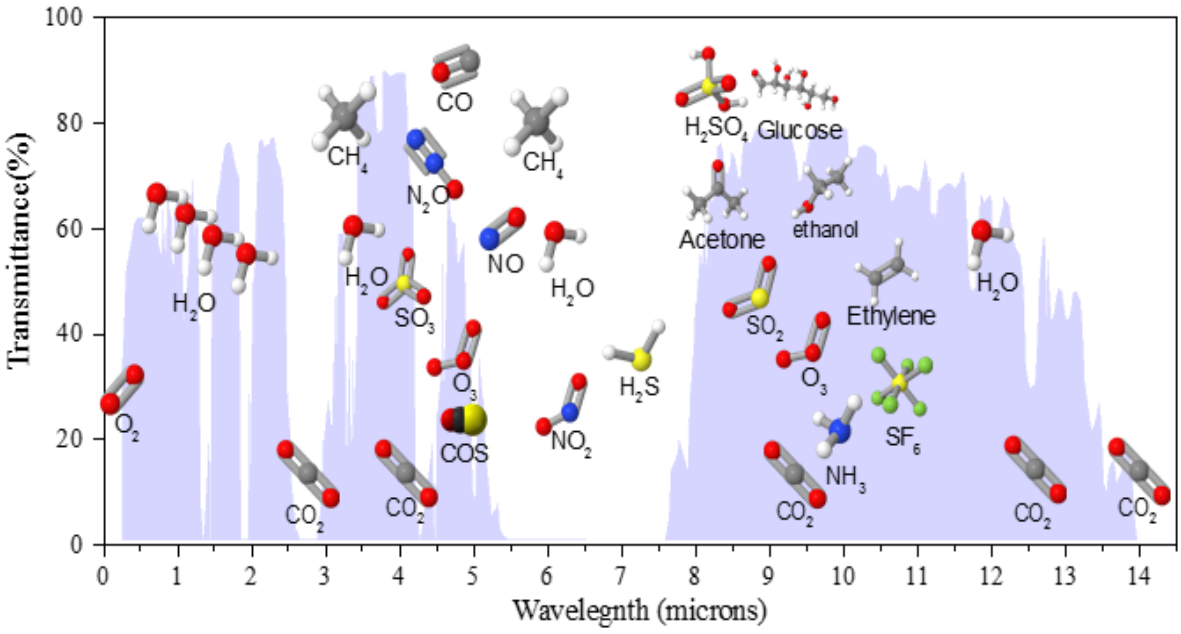

Figure. 2. 1 Atmospheric transmission spectrum from the visible to the infrared. Overlaid on this spectrum, we identify the location of molecular primary absorption lines for a wide range of molecules of interest.

Glasses are more amenable to thermal fiber drawing. In particular, chalcogenide glasses (ChGs) have the broadest transmission range among all amorphous materials and can be thermally

drawn into a fiber directly from the bulk material. Commercially available ChG fibers transmit MIR light and are predominantly produced by double-crucible method [91]. However, this manufacturing approach is complex and also limits the attainable fiber structures. Subsequent coating of the all-glass fiber with a polymer adds mechanical protection, but does not solve the perennial issue of ChG fragile nature. The limitations of current MIR fabrication approaches call for new strategies to produce low-cost, green, robust MIR fibers that provide flexibility in the materials choices and the transverse structures achievable. Chalcogenide glasses (ChGs) are well-known for their IR transparency and amenability to thermal fiber drawing, which makes them attractive candidates for IR optical applications up to 12 μm wavelength in the case of for sulfide-based ChGs, to 16 μm for selenium-based ChGs, and 20 μm for Te-based ChGs. However, the transmission range of meter-long fibers is typically narrower than centimeter-thick bulk samples. Table 2.1 lists the typical transmission region of selected IR fibers.

Table 2. 1 The typical transmission range of selected IR fibers

Fiber material	**Transmission range (μm)**	**Reference(s)**
Fluoride glasses	0.5 – 4.5	[91] [92]
Sulfide-based ChGs	1 – 6	[93] [94] [95]
Selenium-based ChGs	2 – 8	[96]
Tellurium-based ChGs	3 – 12	[97]
AgX-based crystals	4 – 16	[98]

2.2 The history of ChG IR fiber and the concept of multimaterial robust IR fibers

The systematic study of ChGs as IR materials started at the middle of the 20th century. In 1950, Frerichs investigated the As_2S_3 glass [99]. Subsequently, As-S ChG fibers with core-cladding structure were fabricated in 1965 by Kapany and Simms [100], who demonstrated a relatively high transmission loss of 20 dB/m at 5.5 μm.

Several Japanese corporations and research agencies [101] [101] [103] [104] [105] [106] [107] [108] [109] [110] (1980s-1990s) continued the early exploration of ChG IR fibers. Several ChG systems [Ge-P-S, As-S, As-Ge-Se, Ge-S, Ge-As-Se-Te-(Tl)] were drawn into fibers with unclad and core-cladding structures [103] [1111] [112] [113]. A UV curable polymer was coated to provide mechanical protection. In addition, fiber bundles [114] [115] [110] consisting of ChG core, Teflon cladding strands were produced that transmit light along short length. The attempt of using Teflon FEP as cladding in the fiber preform level but not add polymer coating after fiber was drawn leave a hint to later scientists in multimaterial fiber field who can bring multiple distinct material in one fiber to offer multifunctionalities. Other than IR light delivery, they also studied the nonlinearity of ChG fibers [116] [117] [118] [119], rear-earth doped ChG fibers for fiber amplifiers applications [109]. Even with such these achievements about ChG IR fiber from 1980s-1990s in Japan, all these companies still did not find an efficient way to produce low-cost, low-loss, robust ChG fiber even with simplest core-cladding structure. However, these pioneering achievements established a good base for coming boom period.

Amorphous Material, Inc. started to manufacture ChGs since 1977, while their ChG fiber was reported in late 1980s [120]. They have extensive studies on ChG from fundamental material

properties to glass production, characterization, lens molding, fibers, and fiber bundles on several important compositions, such as GeAsSe, AsSe, AsS, and As-Se-Te systems. In their history, two systems of glasses were successfully drawn into fiber: AsSeTe and As_2S_3 glass. However, their fiber still suffer from its fragility which results from material properties, even with thin polymer coating. Their broadband As-Se-Te glass fibers have low attenuation at 2 – 11 μm, while As_2S_3 based fibers cover the range from the visible to 8 μm. These fibers can transmit watt-level (< 5W) of CO and CO_2 CW laser light and have been used for chemical analysis. IR image bundles based on As_2S_3 fibers were produced by winding inside a plastic channel glued to the surface of a 10-m-diameter drum [120], followed by thermally shrinking of additional plastic tube around the bundle as a container protecting the fragile fiber from breakage. However, there is no glass cladding in the single fibers while epoxy was served as cladding which limit the IR transmission spectra [120]. Subsequent efforts by The Institute of Chemistry of High-Purity Substances of the Russian Academy of Sciences (1980s-), Université de Rennes 1 (1990s-), Navel Research Labs (1990s-), University of Southampton (1990s-), and University of Nottingham (1990s-) led to the maturation of the ChG fiber field.

Russian researchers have conducted extensive investigations over the last several decades to determine the nature and origin of impurities in ChGs and their effect on glass and fibers optical properties since the 1980s [121] [122] [123] [124] [125] [126] [127] [128]. An initial report by Dianov *et al.* demonstrated the production of MIR fibers in the As-S, As-Se and As-S-Se systems with optical losses lower than 0.1 dB/m, except for several IR absorption bands caused by stubborn impurities [129]. As-S based fibers with core-cladding structure were fabricated in the early 1990s [130]. Using the double-crucible method, Churbanov *et al.* fabricated core/clad As-Se-Te and As-

S-Se glass fibers with minimal optical losses of 0.15 dB/m at 6.6 μm and 0.06 dB/m at 4.8 μm, respectively [131]. To date, the lowest loss for ChG-based optical fibers have been achieved in multi-mode As_2S_3 optical fibers, with losses of 0.012 and 0.014 dB/m at 3.0 and 4.8 μm, respectively [132].

Start from late 1980s, scientists at Université de Rennes 1 continuously reported their progress about Te-ChG studies, especially for tellurium halides (TeX, X=Cl, Br, I) [133] [134] [135] systems, for fibers. Later on, mono-index and core-clad fibers [136] [137] [138] [139] were produced by both rod-in-tube (directly at the Université de Rennes 1) and double-crucible methods (indirectly from their coworkers). These TeX fibers presents wider transmission widows than S- and Se-ChG, typically up to 9 — 9.5 μm [136] [137] [138] [139]. 2.6 Watts output power is obtained from 1-m-long, 600-μm-diameter unclad TeX fiber with antireflection coating from 7 Watts input power at 9.3 μm wavelength [139]. In additional to energy delivery, TeX fibers are also used for remote chemical analysis and remote temperature sensing [140]. Furthermore, GaSbGeSe-based fibers are also studied since these fibers have higher work temperature than TeX system and better mechanical properties, even they have smaller transmission window [141] [142]. The minimum optical loss of unclad Te-ChG fibers based on TeAsSe system were less than 0.1 dB/m at certain wavelength in the region of 6.7 – 7.3 μm based on TeAsSe glass system [143]. Typical single mode TeAsSe fibers with core-clad structure have the minimum losses ~ 0.33 dB/m at 7.5μm [144]. Broadband step-index Te-ChG fibers possess higher loss (7 — 40 dB/m at 4.0 – 15.0 μm region) are produced by rod-in-tube approach for Darwin mission [145] [146] [147] [148].

U.S. Naval Research Laboratory (NRL) started to report their results about IR ChG fibers on several glass systems [149] [150] [151] [152] [153] [154] [155] [156] [157] [158] [159] [160]

[161], such as AsS, AsSeS, AsSeTe, and GeASSeTe, from unclad fibers to core-clad fibers, microstructure fibers since 1990s. Followed by early Japanese exploration on ChG-core, Teflon-cladding fibers, rod-in-tube approach is initially chosen to produce core-cladding fibers. Attempt to remove the interfacial gap (< 100 μm) between rod and tube, a shrinkable Teflon tube was subsequently used as jacket in the preform level under vacuum at ~100 °C [161]. The fiber core, cladding and Teflon jacket diameters were 200, 330, and 370 μm, respectively with minimum loss less than 1 dB/m at 4.8 μm wavelength. Unfortunately, this single drawing process cannot produce a small core fiber for single-mode confinement and the thin Teflon is not strong enough to offer superior mechanical protection. The core-cladding dimensional ratio is limited by the fabrication methodology of glass tube, which is produced by rotation where only relative thin-wall tube can be obtained. A 1-m-long piece of the same fiber was tested with 6.2 W of CW input power at 5.4 μm from a CO laser. Fiber core diameter was 200 μm, cladding diameter was 330 μm, and peak input-power density was 126 kW/cm^2. Transmission efficiency was 60%, although after a few minutes at peak power the epoxy surrounding the input end face in the connector began to melt [162]. Single-mode ChG fibers were fabricated by a double-crucible technique with 12 μm-core, 125 μm-cladding and ~ 250 μm-UV curable acrylate, as the double-crucible process enables adjustments to be made in the core/clad diameter ratio during fiber drawing by independent pressure control above each melt. The typical loss in this work is about 0.9 dB/m at 2.7 μm wavelength [150]. Rare-earth doped ChGs and fibers for active application in NIR and MIR are also studied extensively at NRL since 1998 [163] [164] [151] [152] [165] [166] [167] [168]. They are also recognized for their commercialization of ChG fibers.

Polymers/plastics/resins generally have been used as coatings (typically UV Acylate) to

offer mechanical protection to fragile glass fibers for several decades [30]. Such protection is critical for ChGs fiber, which only possess 1/10 the tensile strength of silica glass fibers [169]. To overcome this drawback, several approaches have been explored, including the coating with a combination of multiple polymer layers [170], providing a jacket by heat-shrink, and more recently thick built-in jacket through multimaterial coextrusion [62] [171-Te-ChG] on the surface of ChG core and cladding structure, all of which result in better mechanical support compared to single material coating.

The idea of combining glasses with polymers in an optical fiber has been investigated since the 1980s [172] [173] [174] in order to appropriate the favorable mechanical properties of polymers to compensate for the less-favorable mechanical properties of fluoride and chalcogenide glasses. Thermal co-drawing of these glasses with polymer jacket, such as Teflon, greatly improves the mechanical properties of the fiber. In 1981, Shibata and Manabe reported the fabrication of fluoride-glass-core polymer-cladding fibers [175] from a rod-in-tube preform. In 1984, NTT scientists [176] reported similar research using ChGs. Infrared fiber bundles were fabricated using the stack-and-draw approach by Horiba Ltd [177] [178] in the 2 – 6 μm spectral window; see also Refs. [179] [180]. The Naval Research Laboratory (NRL) [181] also developed glass/polymer multimaterial-fiber fabrication technology using the rod-in-tube method in the 1990s. The ability to combine different optical glasses in a fiber and exploiting the contrast in their optical properties can be beneficial in dispersion control and engineering the fiber optical nonlinearities. A fiber consisting of a chalcogenide glass core in a tellurite glass cladding (produced by the stack-and-draw method) [63] [182] [183] was shown to have flattened chromatic dispersion and a zero-dispersion wavelength shifted to the near infrared, enabling supercontinuum

generation covering 800 – 2400 nm. Additionally, all-solid PBG-guiding PCF's consisting of a hexagonal lattice of high-index soft-glass strands embedded in a low-index soft glass [184] (produced by the stack-and-draw method) have been investigated. In practice, this approach is limited by the availability of pairs of glasses with overlapping softening temperatures and thermal expansion coefficients. More research is needed to fully exploit the opportunities enabled by these multimaterial optical fiber structures.

The material processing of bulk material to fiber preform and the fiber drawing process can rarely further improve the purity of material but likely introduce more extrinsic impurities. For example, drilling of glass tube that used as preform cladding usually introduce micron-scale cracks and impurities in the material. Thermal-based preform fabrication and fiber drawing process will also possibly introduce oxidation, therefore, increase the fiber loss. Non-perfection of fiber structure, such as imperfection defects and deformations in core-cladding structure fiber [181], solid-core photonic crystal fiber [182] [183], and 1D [184] and 2D [185] photonic bandgap fibers result from construction of fiber preform and fiber thermal drawing process. Fortunately, for short-haul applications, the mechanical robustness, thermal and chemical stabilities of ChG IR fiber are not far away from practical fiber applications.

The microstructure optical fiber (MOF) technology offers a great controllability of fiber structure design, typically from just a single material (e.g. Silica), where there is no need of two or multiple thermally, chemically, and optically compatible materials to form core and cladding to guide light as conventional fibers. Silica glass have limited adjustment of refractive index by doping, therefore, structure engineering of fiber cross-section provides multiple unique functionalities over simple core/cladding silica fiber. As to ChG, material itself has a huge range

of refractive indices from 2.1 to 3.5 in MIR region, it is not absolute necessary to produce labor consuming microstructure fibers, unless hollow core bandgap ChG fibers which can be used for single mode confinement. Generally, structure engineering of core/cladding fiber, such as thermal tapering process, can easily control the dispersion of fibers. Here in my dissertation, I would not discuss more details about microstructured chalcogenide glass fibers but focus on simple core-cladding structure ChG fibers.

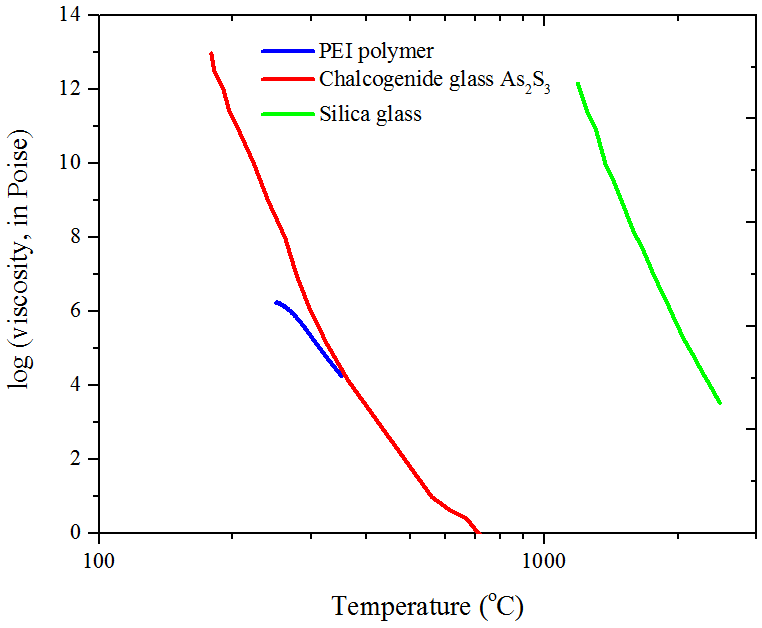

Figure. 2. 2 Viscosity curves of silica glass (green line), chalcogenide glass As_2S_3 (red line) and Polyethylenimine (PEI) polymer (blue line).

Viscosity is the most important parameter in the thermal fiber drawing process. Figure 2.2 is the viscosity curves of three materials: silica (green), ChG As_2S_3 (red) and PEI polymer (blue). Compared with silica, the viscosity of ChG is much more sensitive with temperature, which means difficulties in the thermal drawing process. Fortunately, PEI polymer has similar viscosity curve as ChG in the fiber drawing viscosity region. What if we combine PEI polymer with ChG in the

preform level and then co-draw them together to take the advantage of polymer as scaffold of ChG? This is the initial idea of our multimaterial robust ChG IR fibers. Based on this strategy, we recently developed several novel fabrication techniques that rely on multimaterial coextrusion of specially designed billets combining a thermally compatible polymer with ChG discs to produce a preforms which are subsequently drawn into a robust IR fibers incorporating a thick built-in polymer jacket. The jacket does not participate in the optical functionality but instead offers superior mechanical protection.

2.3 High-purity chalcogenide glass production and preform extrusion

Bulk ChG glasses are mostly prepared by the conventional melt-quenching technique. To get high-quality ChGs without impurities, the melting process must be carried out in the absence of any oxygen or water. ChGs are normally prepared from elements and compounds that have incongruent melting points, exhibit high partial vapor pressure during melting and are susceptible to oxidation and hydrolysis. Therefore, the synthesis must be carried out in sealed evacuated quartz ampoules. High-purity (99.999%-99.9999%) raw materials must be used for the major constituents. ChGs need to be agitated to promote mixing and homogeneity during the melt-based processing. This typically involves the use of a rocking furnace to agitate the melt as the elemental constituents react to form a glass liquid. The primary contaminants ([O], [H], [C] and dissolved compounds) may largely be attributed to trace-level constituents in starting raw materials. These impurities have a noticeable impact on the properties of the drawing of optical fibers. Despite the wide range of ChGs available, only a subset of thermally stable glasses are useful for thermal fiber drawing.

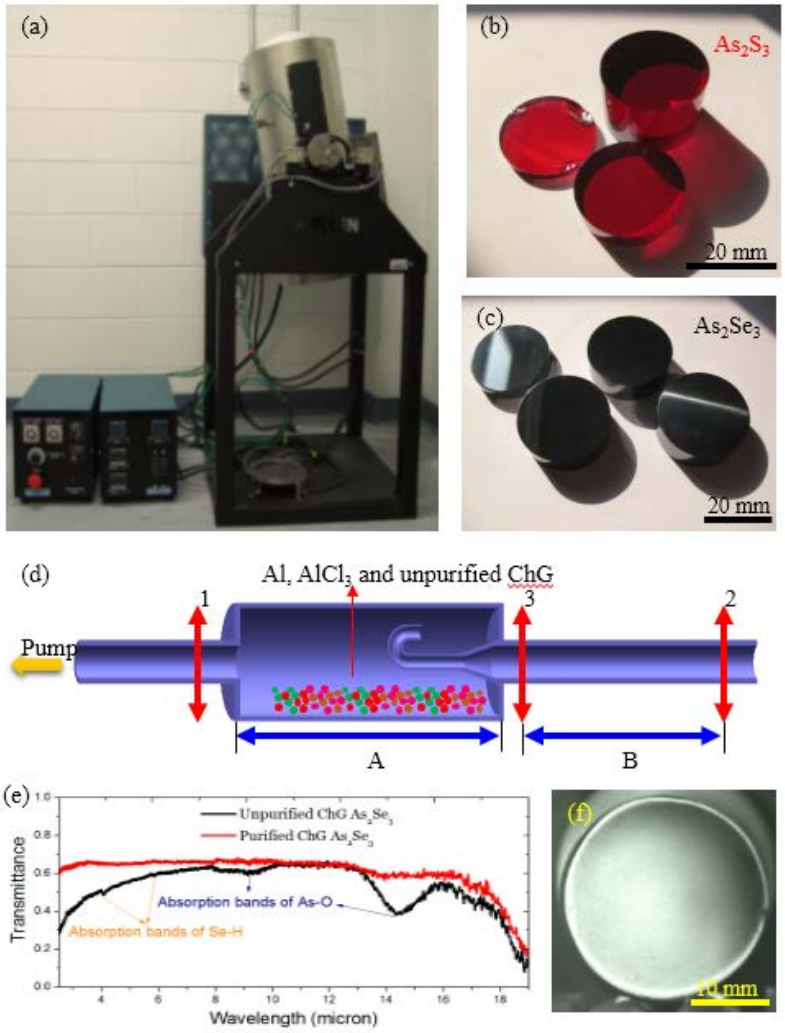

Figure. 2. 3 High-purity, large-scale ChG production ability at CREOL, The College of Optics & Photonics. (a) — (b) Photographs of 30-mm-diameter As_2S_3 and As_2Se_3 ChG discs. (c) The homogeneity of As_2Se_3 glass disc with 10-mm thickness and 30-mm diameter. (d) The comparison of FTIR transmission spectra for unpurified (black line) and purified (red line) As_2Se_3 glass in the form of 10-mm-thick diss. High-purity, large-scale ChG production. (a) A photograph of the rocking furnace used for ChG synthesis. (b) Schematics depiction of the dynamic glass distillation process to produce high-purity ChG.

Bulk quantities of ChGs are usually prepared by cooling of melts. In order to obtain high-quality ChG without any [O] and [H] impurities, the melting process must be carried out in absence of oxygen and water. In general, ChGs are formed by combining elements that have incongruent melting points, may exhibit high partial vapor pressures during melting, and are susceptible to

oxidation and hydrolysis. Therefore, the synthesis must be carried out in sealed evacuated quartz ampoules. The synthesis conditions are widely varied and depend on the glass composition, glass-forming region, and glass-forming ability. High purity (5N – 6N) raw materials are used as initial materials for major elemental constituents. Oxygen [O] is by far the most detrimental contaminant. Elements that are easily oxidized, such as arsenic (As), should be packaged in argon when supplied. Before loading the raw materials into quartz tubes, they should be carefully cleaned.. Next, the temperature of the elements-mixture is raised to form the glass, which must be agitated to promote mixing and homogeneity during the melt-based processing. This typically involves the use of a rocking furnace. Additional steps (such as glass distillation) are usually required to further improve the purity of the glass.

Figure 2.3 shows an example of the high-purity, large-scale ChG production ability at CREOL, The College of Optics & Photonics. Using the approach just described, two 30-mm-diameter discs from well-studied ChGs – As_2S_3 and As_2Se_3 were produced and are shown in Fig. 2.3(a-b). The homogeneity of the glasses is confirmed in Fig. 2.3(c) by near IR light transmission. Figure 2.3(d) compares FTIR transmission spectra of unpurified (black line) and purified (red line) As_2Se_3 glass in the form of 10-mm-thick discs. Based on our self-developed purification techniques for both the raw materials and the synthesized glass [unpublished], we have been able to remove the most stubborn impurities in ChGs.

ChG fibers with core/cladding structure are typically produced by the double-crucible method or the rod-in-tube method. The double-crucible approach is an operationally complex process (and thus out of reach of academia) but typically produces low-loss fibers. However, it produces a limited range of fiber structures and is amenable to a limited choice of materials

pairings for the core and cladding. The rod-in-tube method is a straightforward approach to producing core/cladding fibers. However, such fibers usually exhibit a relatively higher optical loss than those produced by the double-crucible method due to imperfections at the core/cladding interface.

Extrusion can be used to create extended objects with complex cross-sectional profiles by pushing a softened material through a die at suitable temperature under pressure. As shown in Fig. 2.4(b), bulk material, typically called a billet, is placed inside a sleeve and heated to the material's softening temperature. Pressure is used to push the material through a die that imparts shape to the extruded preform rod. Figure 2.4(a) is a photograph of a Ge-Sb-Se ChG rod having a 50-mm diameter and ~75-mm length. Such a ChG rod may be used as an extrusion billet, resulting in a ~1.3-m-long 12-mm-diameter extended ChG rod as shown in Fig. 2.4 (c). The die was a circle of 12-mm-diameter. This is the first demonstration of meter-long extruded ChG rods. This process can be used to reshape large-scale bulk glass into smaller-sized rods with desired cross-sections and extended lengths. Such lengths cannot be produced directly by melt-quenching. Applications in soft-glass lens molding or the fabrication of other IR optical components may benefit from the availability of such extended rods. When compared to the extrusion of polymers and other soft glasses, there have been very few published reports on the extrusion of ChGs. Figure 2.4(d) shows several examples of extruded rods and tubes from GaSbSe, AsS, AsSe glass systems. The hollow tubes are prepared by modifying the die structure by adding a suspended needle in the center of the die13. Extrusion may be also used to produce uni-material complex microstructure optical fiber preforms, as shown in Fig. 2.4(d).

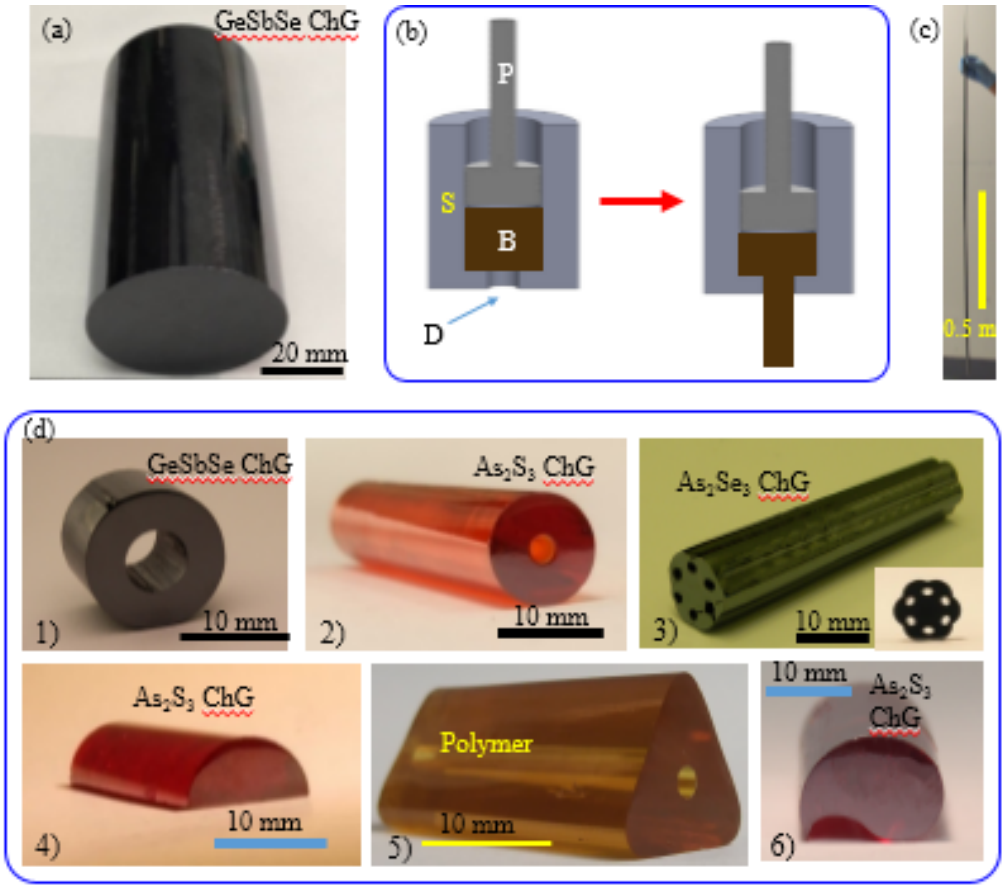

Figure. 2. 4 . Large-scale ChG billet extrusion for meter-long rod. (a) Photograph of a ChG bulk cylinder of 50-mm diameter and ~75-mm length that may be used as an extrusion billet. (b) Schematic of rod extrusion from a single material. (c) Photograph of extruded ChG rod with ~1.3 meter length and ~12 mm diameter produyced from the billet in (a). (d) Examples of extruded structures and materials. From left to right: hollow GeSbSe tube, hollow As_2S_3 tube, and six-hole As_2Se_3 PCF preform

Combining multiple materials in a fiber may be used to improve the mechanical properties lacking in a fiber that has favorable optical properties. As mentioned above, while chalcogenide glasses have high optical nonlinearity and are transparent in the mid-infrared, the adoption of chalcogenide fibers has been limited due, in large part, to their unfavorable mechanical properties. This drawback has been recently addressed through the use of one-step multimaterial coextrusion of a fiber preforms containing chalcogenide glasses and thermoplastic polymers. A composite preform consisting of a Chalcogenide glass core, a chalcogenide glass cladding, and a built-in

polymer jacket is extruded from a vertically stacked billet into a preform that is subsequently drawn into a fiber. The polymer provides protection to the fibers during drawing and mechanical handling after drawing. Furthermore, since the chalcogenide glass and the polymer are thermally compatible, the fiber may be tapered without removing the polymer, resulting in robust, all-solid, and high-index-contrast tapers with sub-micron core diameters. These tapers have been used to produce octave-spanning infrared supercontinuum spectra.

2.4 Multimaterial stacked coextrusion for robust ChG IR fiber production

In this Section, I summarize our multimaterial stacked coextrusion technique, which produces composite ChG/polymer preforms that are then drawn into robust fibers. A billet consisting of thermally compatible thermoplastic polymer and ChG is extruded into a preform provided with a built-in polymer jacket. The polymer does not participate in the optical functionality of the fiber, which is dictated by the ChG alone. We also produce robust, high-index-contrast, sub-micrometer core-diameter tapers suitable for nonlinear optical applications without removing the polymer.

Our extrusion system consists of a sleeve (diameter 30–46 mm) inside a tube furnace. A billet is heated in the sleeve to allow viscous flow and is then extruded by a piston through a circular die [diameter 6–20 mm; Fig. 2.5(a)]. The billet is kept at slightly higher than the softening temperature, and ≈500 lbs of force is applied to extrude the billet at ∼0.3–0.7 mm⁄min. Extrusion under pressure allows the use of lower temperatures and higher viscosities compared to fiber drawing, thereby reducing glass crystallization.

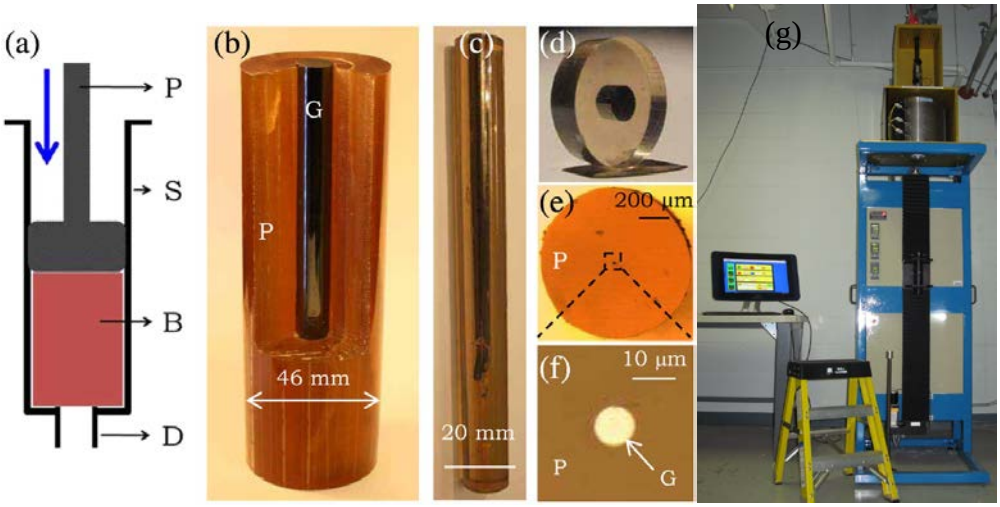

Figure. 2. 5 (a) Extrusion system. P, piston; S, sleeve; B, billet; D, die. (b) A hybrid polymer (P: PES) and ChG (G : As_2Se_3) billet. A section of the polymer was removed to reveal the structure. (c) Section of the extruded preform. (d) A disk (diameter 17.4 mm) cut from the extruded preform in (c). (e) Reflection optical micrograph of the fiber cross section and (f) the core. (g) Photograph of extruder in CREOL, UCF

ChG rods were prepared from commercial glass (AMI, Inc.) by melt quenching, and polymer rods were prepared by thin-film processing. The glasses used are G_1:As_2Se_3, G_2: $As_2Se_{1.5}S_{1.5}$, and G_3:As_2S_3, with measured indices 2.904, 2.743, and 2.472 at 1.55 μm, respectively; the polymers used are polyethersulfone (PES) and polyetherimide (PEI). The large index contrast between the ChGs was chosen to test the limits of the extrusion process and to produce the high-index-contrast nanotapers described below. As a first example, we extrude a ChG-core (G1), polymer-jacket (PES) preform [Figs. 2.5(c) and 1(d)] using a nested billet consisting of a ChG rod (11 mm diameter, 60 mm length) in a polymer tube [46 mm outer diameter, 140 mm length; Fig. 2.5(b)]. We refer to this structure as GP.

We next extrude a preform with a ChG cladding surrounding the ChG core. We use a vertically stacked billet comprising polished disks placed atop each other with the bottom (top) disk corresponding to the outermost (innermost) layer in the extruded preform [Fig. 2.6(a)]. The

extruded preform consists of nested shells with the top-billet layer forming the core. We refer to this structure hereafter as GGP. The polymer protects the ChG from coming in contact with the die during extrusion or subsequently with the ambient environment. We do not observe any separation between the layers in the preforms (or in the subsequently drawn fibers). The larger thermal expansion coefficient of the polymer compared to the ChG eliminates in the preform the small gaps that inevitably exist at interfaces in the billet.

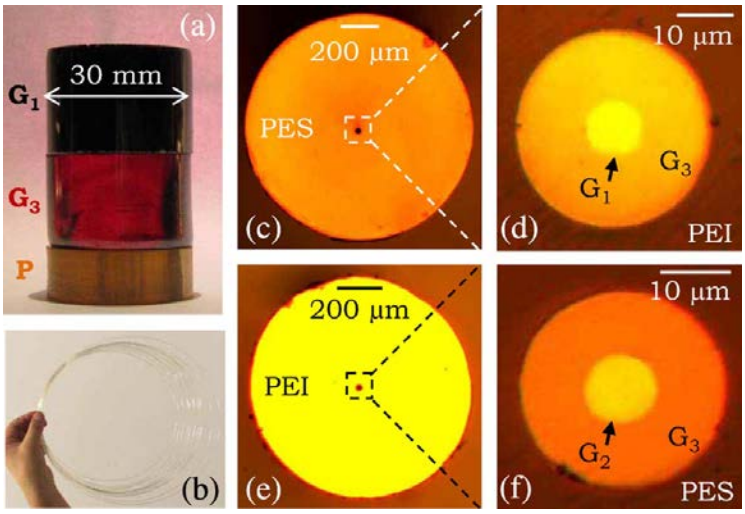

Figure. 2. 6 (a) Vertically stacked billet to produce a GGP preform. (b) Drawn GGP fiber. (c), (e) Transmission optical micrographs of the fiber cross sections, and (d), (f) reflection micrographs of the core. P, polymer; G_1:As_2Se_3, G_2:$As_2Se_{1.5}S_{1.5}$, and G_3:As_2S_3.

We draw each preform into a cane, and a 10-cm-long section of it is inserted into a polymer tube, which in turn is drawn into ≈100 m of continuous, robust, 1-mm-outerdiameter, 10-μm-core-diameter fiber [Fig. 2.6(b)]. Cross section of the GP fiber is shown in Figs. 2.5(e) and 2.5(f), and cross sections of two GGP fibers, G1–G3–PEI and G2–G3–PES, are shown in Figs. 2.6(c) and 2.6(d) and Figs. 2.6(e) and 2.6(f), respectively. The ChG in the latter two represents less than 0.1% of the fiber volume: 10 km of this fiber contains ~30 g of glass. The core-to-cladding diameter ratio here is ≈1⁄3. This ratio is controlled by changing the thicknesses of the disks in the billet and

the pressure applied during extrusion. Reducing this ratio, however, reduces the yield of the useful preform length. The built-in polymer jacket facilitates the fiber drawing compared to bare-glass-fiber drawing and helps avoid oxidation of the ChG. The fiber transmission losses (for a GGP fiber with As_2Se_3 core) evaluated by cutback measurements are ≈10:9 dB⁄m at 1.55 μm (using a laser diode) and ≈7.8 dB⁄m at 2 μm (using a Tm-doped fiber laser). The loss at the moment is limited by the purity of the glass.

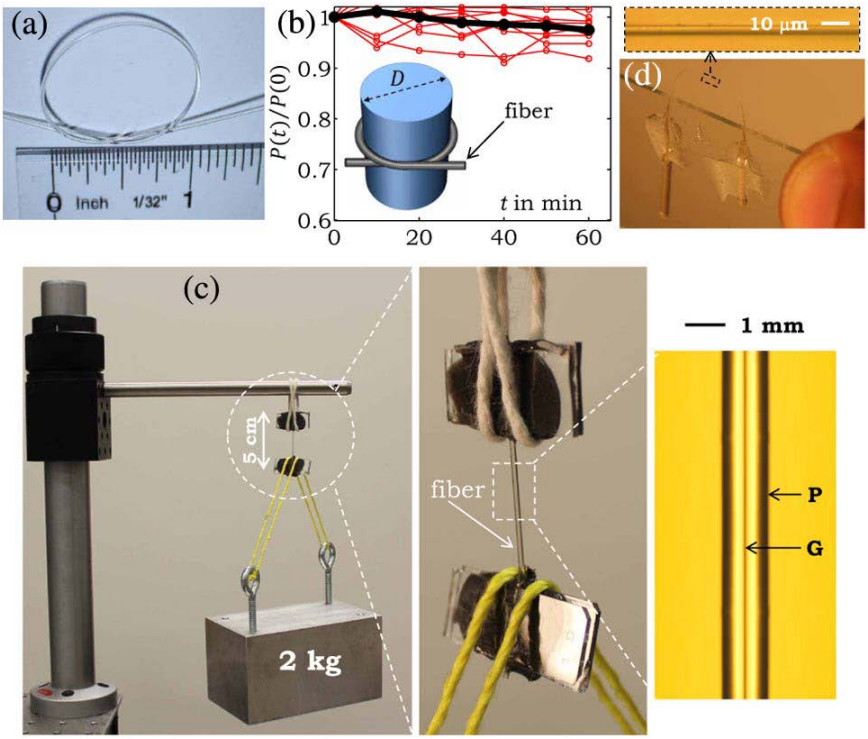

Figure. 2. 7 (a) A 1-mm-diameterfiber tied in a 1-in.-diameter knot. (b) Transmission over time for 10 fibers after bending the fiber with D ~ 0.5 in: bend diameter. The black curve is the average of all the measurements. (c) A 2 kg weight hanging from a 5-cm-long fiber. The inset shows the hanging mechanism. The fiber is attached to microscope slides using epoxy while keeping the ends free for optical measurements. (d) A robust multimaterial taper. The inset is a micrograph of the taper center.

The robustness of these composite ChG fibers is illustrated in Fig. 2.7.We measured the transmission over time (at 1.55 μm) after bending a GP fiber for 10 min intervals. There was no change for 1 in. bend diameters and larger, and we find no plastic memory in knots with diameters

larger than 1 in. [Fig. 2.7(a)]. Results for a 0.5 in. bend diameter are plotted in Fig. 2.7(b). The transmission did not decrease after an hour by more than 10% (5% on average). We also investigated the effect of axial stress on optical transmission. We hang a 2 kg weight from multiple 5-cm-long GP fiber sections [Fig. 2.7(c)] for 18 h each and then measure the transmission (at 1.55 μm): it was unaffected in this experiment. The fiber thus withstands 14.6 Kpsi (≈25.5 MPa) with no change in its performance over this extended period of time. This sets a lower limit on the fiber strength. Although the ChG diameter here is only 10 μm, the polymer jacket nevertheless allows for convenient handling and reduced ageing of the fibers. Therefore, the optical properties of the fiber are determined by the ChG, while the mechanical properties are determined by the polymer. Separating the functionalities in this way allows for them to be optimized independently.

A unique advantage of the thermally compatible builtin polymer jacket is in providing a mechanical scaffold for producing robust tapers without first removing the polymer. ChG nanotapers combine high optical nonlinearities with dispersion control but are hampered by their extreme fragility. The robustness of our multimaterial tapers is highlighted in Fig. 2.7(d), where we show a taper with core diameter 25 nm (outer diameter 3 μm).

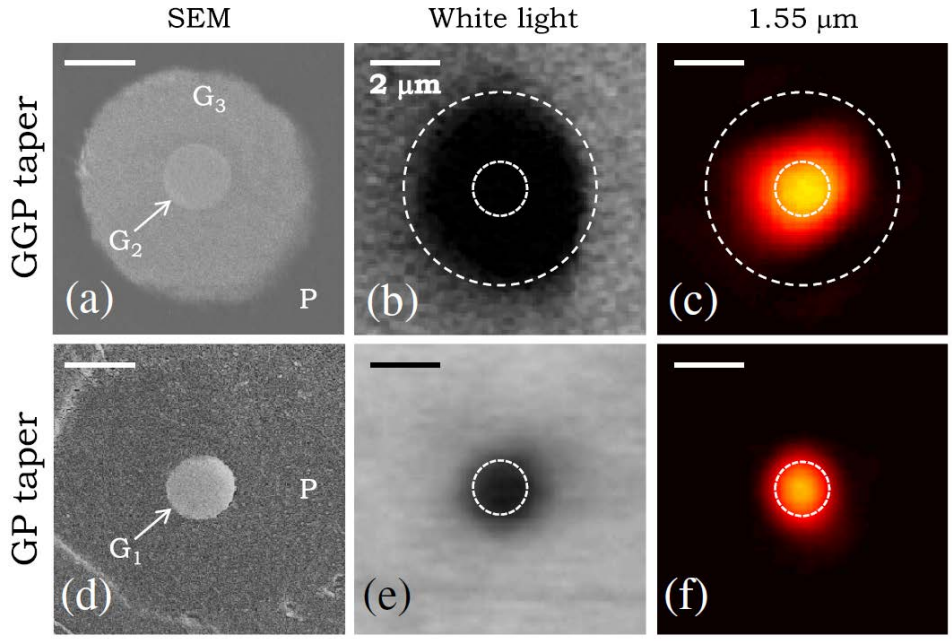

Figure. 2. 8 (a)–(c) Characterization of GGP and (d)–(f) GP tapers both having core d_{min} =1.4 μm. (a), (d) SEM micrographs of the cross sections; (b), (e) white-light and (c), (f) 1.55 μm laser light near-field intensity images. Scale bars are 2 μm. Dashed white circles corresponding to the interfaces are guides for the eye.

We characterize GP and GGP tapers in three ways after cutting the taper at its center where the diameter is smallest (d_{min}=1.4 μm for the core in both tapers). (1) The structure is determined using scanning electron microscope (SEM) imaging, confirming that size reduction occurs at the same rate throughout the cross section during tapering [Figs. 2.8(a) and 2.8(d)]. (2) The ChG-polymer interface is determined by transmitting white light (coupled from the untapered end, do _ 10 μm), since the polymer We characterize GP and GGP tapers in three ways after cutting the taper at its center where the diameter is smallest (d_{min}=1.4 μm for the core in both tapers). (1) The structure is determined using scanning electron microscope (SEM) imaging, confirming that size reduction occurs at the same rate throughout the cross section during tapering [Figs. 2.8(a) and 2.8(d)]. (2) The ChG-polymer interface is determined by transmitting white light (coupled from the untapered end, d_o = 10 μm), since the polymer is transparent in the visible and the ChG is not

[Figs. 2.8(b) and 2.8(e)]. (3) The modal structure is determined by transmitting 1.55 μm CW light (from a laser diode) through the core [Figs. 2.8(c) and 2.8(f)]. The mode is confined to the glass in the GGP taper owing to the high core/ cladding index contrast (and extends into the polymer in the GP taper). We thus harness the mechanical strength of the polymer jacket without compromising the optical functionality of the taper.

In conclusion, we have described a novel one-step multimaterial preform extrusion process that produces hybrid ChG/polymer preforms that we draw into robust infrared fibers and tapers. The process helps obviate the mechanical limitations of ChG fibers and enables optimizing the optical properties for nonlinear applications.

2.5 Multimaterial coextrusion of preforms for 'disc-to-fiber' production

The billet in Fig. 2.6(a) requires the use of 30-mm-diameter ChG discs, which requires large-scale synthesis of high-purity glass. Such a task is not easy in an academic setting, and thus limits access to other research groups from attempting such a process. Furthermore, the extruded preform is characterized by an internally tapered structure, and thus only a small percentage (~ 5 – 10%) of the materials used is converted into the desired transverse geometry. In this Section, we bring forth a modification of the previously reported multimaterial coextrusion strategy that offers a two-fold improvement. First, only a very small quantity of glass is required in preparing the extrusion billet. Indeed, we demonstrate that using two glass discs with 10-mm diameter and 3-mm thickness (~ 2 g total mass) is required to produce a preform that is drawn into ~ 50 m of continuous fiber. Furthermore, a higher percentage (~ 25%) of the material is utilized in the drawn

fiber. The result is an efficient methodology that in effect converts glass discs to step-index fibers (that we call a ‘disc-to-fiber’ approach) with core diameters in the range of tens of microns. The small quantity of glass requires helps simplify the demands on large-scale glass production and expedites the evaluation of candidate glasses as potentially viable fiber materials. The combined capabilities of producing high-purity, large-scale ChGs discs with our multimaterial fiber fabrication strategy2 lead to the production of robust, low-loss IR ChG fibers with the desired dimensions and refractive index contrast between core and cladding.

Using a vertically stacked billet constructed of discs from the desired materials, the horizontal interfaces are converted during extrusion to vertically nested interfaces. The extruded rod therefore form nested concentric structure, such as core-cladding structures or one-dimensional (1D) multilayered structured preforms. In 1994, K. Itoh et. al. reported the use of extrusion to produce a core/cladding fluoride preform directly by stacking two discs in a billet [186]. After this pioneering result, A. B. Seddon’s group at Nottingham University[187] [188], J. A. Harrington’s group at Rutgers University[60], and D. J. Richardson’s group at Southampton University [61] used a similar approach to use multiple discs to produce step-index or 1D microstructured fiber preforms.

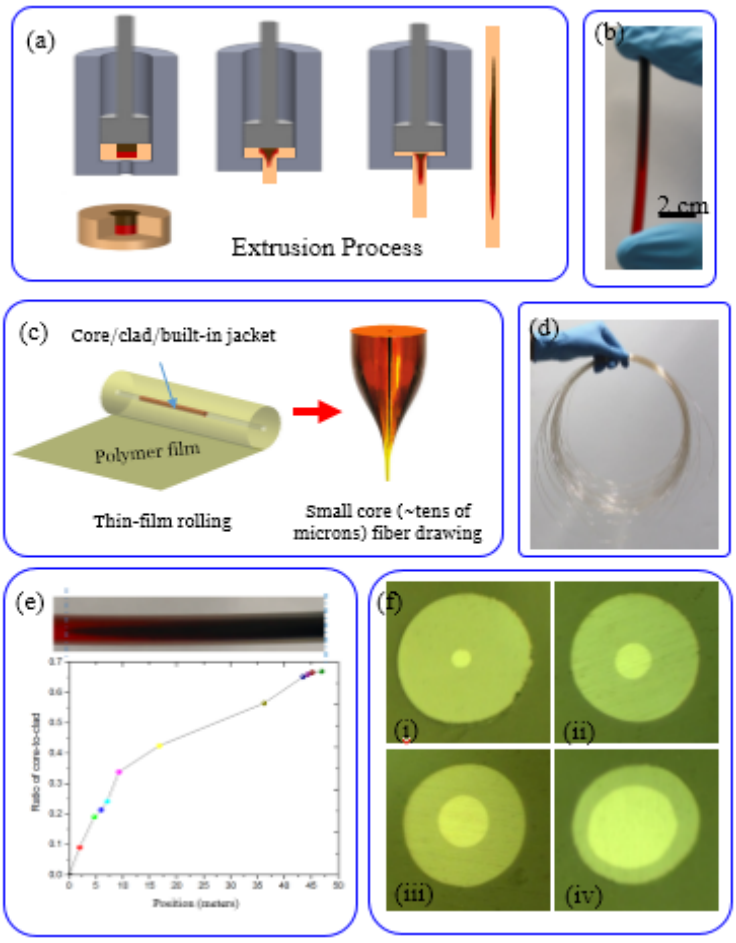

Figure. 2. 9 (a) Schematic of efficient 'disc-to-fiber' coextrusion. (b) Photograph of part of the extruded rod resulting from the billet with the structure shown in (a). (c) Drawn fiber produced from the preform in (b). (d) Ratio of core-to-cladding in the fiber versus the location of measured point along the fiber. (e) Optical reflection micrographs of fiber cross-sections showing different core-to-cladding diameter ratios $d_{core}/d_{cladding}$: (i) 5.92/65.2 μm; (ii) 11.3/52.8 μm; (iii) 20.5/50.2 μm; (iv) 27.6/41.9 μm.

We recently reported a modification of this strategy that allows for combining heterogeneous materials in the billet – a multimaterial stacked coextrusion strategy5. We used a multimaterial billet consisting of vertically stacked discs, which allows for engineering the transverse architecture of the extruded rod that contains a core-cladding structure combined with a built-in jacket. This rod constitutes a preform structure in which the ChGs are protected by the

thermoplastic polymer, which dramatically simplifies the subsequent thermal drawing into a fiber. The main advantage of this process is its ability to create preforms with complex transverse structures from brittle material that may then be drawn into a robust fiber. Several fibers have been drawn from these extruded multimaterial preforms and have led to the fabrication of robust nano-tapers that enable optical dispersion engineering and nonlinear optical applications in coherent supercontinuum generation.

Since the multimaterial preforms were produced from a stacked billet by converting the horizontal interfaces to vertically nested structure, the extruded preform has an internal tapered ratio of core/cladding diameters, as showed schematically in Fig. 2.9(a). Only a small percentage (5%-10%) of the initial materials is converted into a preform with step-index ChG structure that is useful for fiber drawing. Furthermore, large-diameter discs (30-mm-diameter) were needed in the billet. Here we report on a second generation of multimaterial extrusion that requires significantly less glass (only ~ 2 gm) to produce a robust IR fiber. We call this procedure multimaterial 'disc-to-fiber' coextrusion.

We address these two challenges (the large material quantity needed and the low utilization efficiency) by redesigning the hybrid ChG-polymer extrusion billet structure [Fig. 2.9(a)]. Similarly with multimaterial stacked coextrusion, we produce preforms with step-index ChG preform provided with a built-in polymer jacket. The optical functionality of the drawn fiber is dictated by the ChG, while the mechanical properties stem from the polymer. The billet here was constructed using two 10-mm-diameter 3-mm-thick glass discs, corresponding to only a few grams of glass.ChG discs were prepared by melt-quenching23 from high-purity elements, As, S, and Se (99.999%). The glasses used are G1: $As_{40}Se_{60}$ and G2: $As_{40}S_{60}$ with measured indices 2.904 and

2.472 at 1.55 μm wavelength, respectively. The samples (typically 10 g in weight) were prepared by melting batches in evacuated (10^{-4} Pa) and flame-sealed silica ampoules in a rocking furnace at 900 – 950 ◦C for 12 h, quenching them in cold water to obtain solid ChG for further glass distillation. After distillation, high-purity glass is remelt again for 4 – 6 h, followed by quenching and annealing. Finally, the annealed glasses were cut and polished to mirror smoothness into slices for extrusion. The weight of each glass disc is around 2.5 g. The polymer used is polyethersulfone (PES). The polymer rod used for extrusion was produced by the thin-film rolling technique. The polymer component is now produced in a different form with respect to the first-generation of coextrusion (that is, not the solid disc used previously). Instead, a stepped hole is made with a polymer cylinder in which the two glass discs are fitted. The outer diameter of the polymer rod is 30 mm to fit into a 30-mm-diameter metal sleeve. The billet assembly is heated in the sleeve to the softening temperature of both glass and polymer materials, and is then pushed through a circular die with 4-mm diameter under 300 – 500 lbs of force at ~0.3 – 0.7 mm/min piston downfeed speed. The resulting extruded multimaterial rod is shown in Fig. 2.9(b). An additional advantage of this billet structure is that contact between the glass disc and the metal walls of the extrusion sleeve is eliminated. Therefore, we expect that any contamination of the glass due to such contact at elevated temperatures is reduced.

The extruded multimaterial rod [Fig. 2.9(b)] is then used to produce a preform by increasing its diameter via a thin-film-rolling approach. Thermal drawing of the resulting preform in an ambient environment produces ChG fibers [Fig. 2.9(c)] with tens of microns core diameter, 1-mm outer diameter and ~ 50 m of length fiber containing a step-index ChG structure and built-in jacket [Fig. 2.9(c)], which is a greatly improved production efficiency. In addition, the

thickness-to-diameter dimensional ratio of each glass disc is only 0.3, which is much smaller than that of the first generation extrusion which is around 1. Hence, much more material could be converted into vertical structure, 40 – 50% in this work. Figure 2.9(d) presents the core-to-cladding ratio in the fiber as a function of the distance from the measured position to the beginning of fiber. From these measurements we conclude that useful robust infrared fibers are produced here with 0.09-0.68 ratio of core-to-cladding diameters starting from less than 2 g of glass materials. These fibers have the same excellent mechanical properties as the fibers reported in our previous work in Ref [62]. Figure 2.9(e) depicts optical micrographs of several fiber cross sections taken at different positions along the drawn fiber showing the change in the core-to-cladding diameter ratio.

An efficient disc-to-fiber coextrusion methodology has been described that may help alleviate the challenges of producing high-purity, large-scale chalcogenide glass synthesis, which are obstacles to the development of infrared chalcogenide fibers. Our multimaterial coextrusion approach produces robust infrared fibers using extremely small quantities of glass. We thus expect this process to have substantial impact on the development of a new generation of infrared fibers by providing an efficient route to rapid prototyping of fibers from new materials.

2.6 Multimaterial rod-in-tube coextrusion

The rod-in-tube approach is a straightforward method that is used to produce core-cladding step-index fiber structures from a wide range of materials. Unfortunately, it typically results in fibers with higher transmission loss due to imperfections at the core-cladding interface. Amorphous Te-ChGs not only have broad transmission spectrum cross this range, but also can be

thermally drawn into a fiber directly from a preform. Here we use Te-ChG to produce a robust IR fiber that can transmit radiation in the 3 – 12 μm spectral range.

Table 2. 2 Optical properties Te-based chalcogenide core/cladding fibers

Glass composition	Spectral range (μm)	Lowest loss (dB/m)	Wavelength (μm)	Reference
$As_3Se_{4.5}Te_{2.5}/As_3Se_5Te_2$	2 – 12	1.7	6.5 – 9.5	[190]
$Ge_{21}Se_3Te_{76}/Ge_{21}Se_8Te_{71}$	4 – 15	20	4 – 15	[191]
$Ge_{20}As_{20}Se_{16}Te_{44}/Ge_{20}As_{20}Se_{18}Te_{42}$	5 – 12	3 – 4	6 – 10	[192]
Te-X (X = Cl, Br or I)	3 – 13	1 – 2	7 – 10	[193]
$Se_{3.9}As_{3.1}Te_2I/Se_4As_3Te_2I$	3 – 13	1	5-9	[194]

Since then, several ChG fibers have been developed, including Te-ChG fiber. Unclad Ge-Se-Te glass fibers were reported in the 1980's[189]. More recently, Te-ChGs were drawn into unclad and core-cladding fibers, including As-Se-Te[190], Ge-Se-Te[191], Ge-As-Se-Te[192], Te-X (X=Cl, Br, I)[193], and Se-As-Te-I[194] glass systems. Table 3.1 summarizes the characteristics of the Te-ChG fibers reported to date along with the core-cladding structure, transmission spectral range, and the lowest transmission loss within the MIR.

Many soft glasses useful for IR fibers have unfavorable mechanical properties. For example, while ChGs have high optical nonlinearities and are transparent in the MIR, the adoption of ChG fibers has nevertheless been limited in large part due to their unfavorable mechanical properties. This drawback has been recently addressed through the use of one-step multimaterial coextrusion of a fiber preform containing ChGs and thermoplastic polymers. A composite preform consisting of a ChG core, a ChG cladding, and a built-in polymer jacket is extruded from a vertically stacked billet into a preform that is subsequently drawn into a fiber. The polymer

provides protection to the fibers during drawing and mechanical handling after drawing. Furthermore, since the ChG and the polymer are thermally compatible, the fiber may be tapered without removing the polymer, resulting in robust, all-solid, and high-index-contrast tapers with sub-micron core diameters. These tapers have been used to produce octave-spanning infrared supercontinuum. However, this stacked extrusion procedure results in a tapered core/cladding preform structure, and thus has a low utilization efficiency of the materials. Here we report a new multimaterial coextrusion technique, multimaterial rod-in-tube coextrusion, which combines elements from the traditional rod-in-tube method with our co-extrusion approach to produce robust MIR fibers.

ChG cylinder rods were prepared by the melt-quenching method; core: $Ge_{20}As_{20}Te_{45}Se_{15}$, cladding: $Ge_{20}As_{20}Te_{42}Se_{18}$. Figure 2.10(a) shows a schematic of our procedure. To prepare the extrusion billet, a cylinder of the core glass G1 (diameter is intentionally tapered in the range 7.92 – 7.95 mm, height = 19.0 mm) was obtained by sectioning and polishing a longer cylinder, while a cylindrical tube (outer diameter = 15.0 mm, inner diameter tapered in the range 7.95 – 8.00 mm, height = 22.0 mm) of the cladding class G2 was obtained by sectioning, mechanical drilling, and polishing the inner tube surface. To reduce the potential gap between rod and tube, both the outer dimension of rod and inner dimension of tube were polished with a slightly tapered structure, as shown in the schematic drawings in Fig. 2.10(a). The rod is inserted into the tube to form a rod-in-tube assembly, followed by inserting it into a polymer cylinder with a stepped hole. The polyethersulfone (PES) polymer rod with a stepped hole (outer diameter = 30 mm, inner diameter = 15.2 mm, depth = 23.0 mm) that fits the rod-in-tube assembly was prepared by the thin-film-rolling technique3 and mechanical machining. The billet was loaded into an extrusion sleeve with

30 mm inner diameter and heated to the materials' softening temperature. The billet was forced through a circular die with inner diameter of 6 mm under 300 – 500 lbs of force at ~ 0.3 – 0.7 mm/min speed to obtain a multimaterial preform with glass core, glass cladding, and polymer built-in jacket structure [Fig. 2.10(b)]. Figure 2.10(c) is a photograph of a section of extruded preform, a section of which is subsequently rolled with additional PES polymer by thin-film-rolling approach to form a large-scale preform with outer dimension ~ 25 mm. A 1-mm-diameter fiber is drawn from the well-consolidated preform in a home-built fiber tower. Figure 2.10(d) shows a 7-m-long section of the drawn fiber. We have thus demonstrated that combining multimaterial coextrusion with the rod-in-tube methodology enables us to approach full-utilization of the materials used, thereby maximizing the yield – without compromising the fiber robustness.

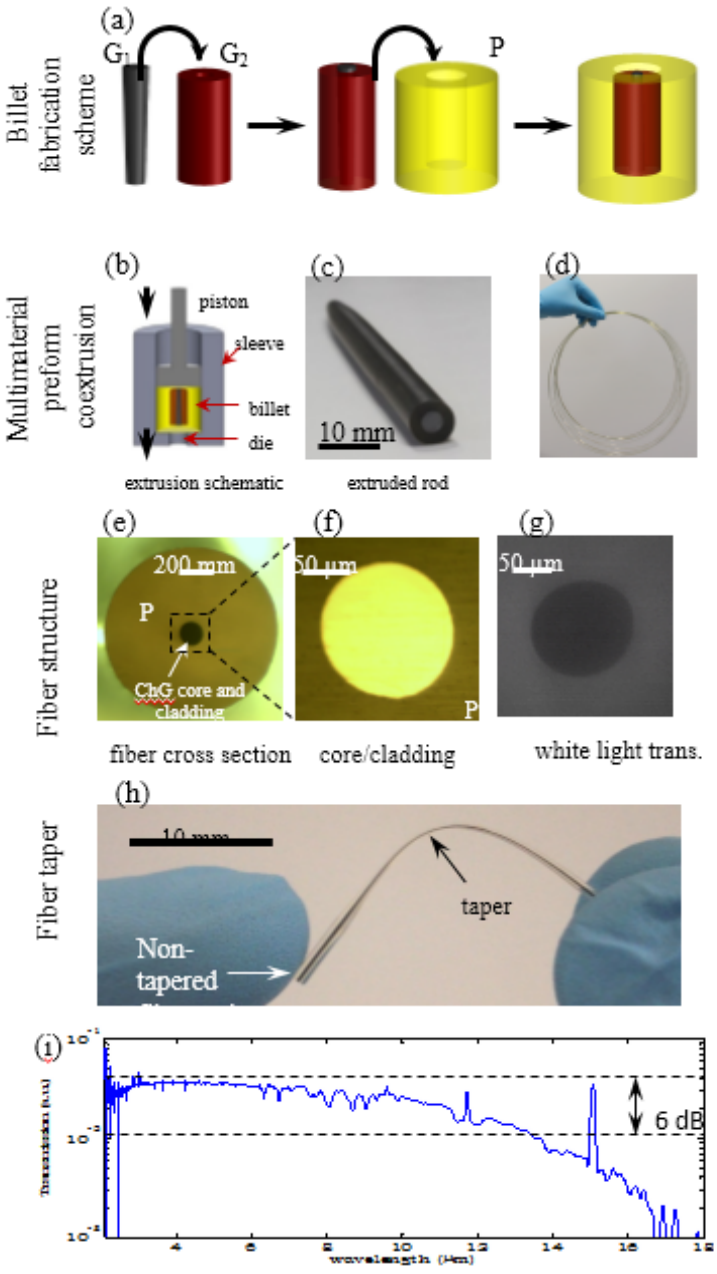

Figure. 2. 10 Fabrication of robust multimaterial Te-ChG fiber. (a) Fabrication steps to produce the extrusion billet via a modified rod-in-tube process, culminating in a hybrid ChG/polymer extrusion billet. G_1 (rod) and G_2 (tube) are the core and cladding glasses, respectively, and P is the polymer jacket. (b) Schematic of the extrusion process. (c) Photograph of the extruded preform with ChG core/cladding structure and built-in polymer jacket structure. (d) A 7-m-long drawn fiber. A transmission optical micrograph of the fiber cross section. (b) A reflection optical micrograph of the core/cladding region corresponding to the dashed square in (a). (c) White light transmission of core/cladding region. The core/cladding interface is not visible due to the small index contrast. (d) A mechanically robust Te-ChG taper. The black-colored core and cladding are visible inside the transparent polymer jacket.

We carried out optical characterization of our fiber using multiple MIR sources throughout the spectral range of interest. The FTIR transmission spectrum for a 3-cm-long fiber sample shows a broad transmission window in the 3 – 12 μm spectral range that is within 6 dB from the peak transmission. Since one of the main applications of such a fiber is in QCL transmission, we measured the fiber loss by the cutback technique using two QCLs at wavelengths 6.1 and 9.4 μm using 1-m-long fiber samples. These measurements yielded estimated losses of 6.1 dB/m and 4 dB/m at these two wavelengths, respectively. The mode profile was determined using a He-Ne laser at 3.39 μm. The measured divergence of the mode emerging from a 20-cm-long fiber corresponds to NA of 0.26 at 6.1 μm.

Uniquely, the thermo-compatible polymer jacket allows for fiber tapering without first removing the jacket. As a result, these fibers may be used to prepare mechanically robust tapers for nonlinear fiber applications in the long-wave MIR spectrum. While there are available chalcogenide fiber tapers for mid-wave wavelengths, the tapers shown here are the first demonstrated for long-wave MIR applications. The fiber taper shows a drop in transmission of less than 50% after reducing the outer diameter from 1 mm to 320 μm over a 10-cm-long sample.

In conclusion, we have demonstrated a novel fabrication approach for producing robust mid-wave and long-wave MIR fibers that makes use of tellurium-based chalcogenide glasses. The multimaterial fiber is drawn continuously from a preform obtained by extruding a rod-in-tube billet assembly. The resulting fiber is robust yet flexible and maintains low loss across the 3 – 12 μm spectral window, thereby making it an attractive prospect for QCLs.

CHAPTER 3 IN-FIBER SYNTHESIS AND IN-FIBER FLUID INSTABILITIES

3.1 In-fiber synthesis

The high-temperatures associated with thermal fiber drawing and the potential of using core and cladding materials with very different chemical reactivity suggests the possibility of exploiting fiber drawing in chemical synthesis. In this context, the preform cladding is viewed as a crucible in which a chemical synthesis process is confined. During fiber drawing, physical changes first take place, such as a reduction in the core and cladding viscosity, and potentially melting or volatization of the core. In the in-fiber synthesis approach, these *physical* changes are then followed by *chemical* changes where new compounds are produced in the core, either by reactions between pre-existing core compounds, or through diffusion of elements or compounds from the cladding into the core. This is an example of a re-imagining of the fiber drawing process itself, where the elongation at high temperature of multimaterial fibers is used to achieve a new goal: controlled chemical reactions along an extended length in confined space.

The multimaterial in-fiber synthesis concept may be traced to work by E. Snitzer and R. Tumminelli in 1989 [64]. The drawing temperature of the fiber was higher than the core soft-glass T_m and its higher vapor pressure in the liquid phase led to the volatization of some compounds in the hot neck-down region resulting in a different residual core composition. This pioneering work can also be viewed as the first instance of drawing two families of materials having incompatible thermal properties.

More recently, low-temperature materials ($Se_{97}S_3$ and $Sn_{85}Zn_{15}$) were co-drawn and a ZnSe compound was produced in the drawn fiber [24]. A surprising feature is that the produced

compound (ZnSe here) has a much higher melting temperature than that of the drawing process. J. Ballato *et al.* [195] used as-purchased crystalline Bi_2O_3-rich (Bi_2O_3 + GeO_2) and $Bi_{12}GeO_{20}$ powders (core) placed in borosilicate glass tube (cladding) to produce fibers where an *in situ* reactive chemical synthesis takes place during the drawing process in both amorphous and crystalline cores. This processing route can be used potentially for core materials that are difficult to fabricate or machine into a rod using conventional methods. Furthermore, in an attempt to reduce the diffusion of oxygen from the silica cladding to the Si core, silicon carbide (SiC) was introduced into the core to provide an *in situ* reactive oxygen getter during the drawing process [196] through the reactive-molten-core method.

3.2 In-fiber fluid instabilities

During thermal drawing, the viscosity of the drawn materials is reduced. A multimaterial fiber preform is thus a complex fluid-dynamical system. In the neckdown region where the diameter of the large preform is reduced to that of the drawn fiber, the constricted flow of the materials may be compared to the flow of a jet out of a nozzle. The controllable reduction in feature sizes within a multimaterial fiber therefore potentially allows fluid instabilities to develop at the heterogeneous interfaces. Although such phenomena are universal and ubiquitous, they lay dormant during the development of traditional silica fibers for several reasons. First, since the core and cladding are very similar materials (usually the same glass with different dopants), there is very little surface energy at the interface. Second, the high viscosity of silica glass helps arrest the development of fluid instabilities. Third, the high drawing speed results in a small dwelling time in the low-viscosity state, which is typically much shorter than instability growth times. Finally, the core diameter is relatively large (hence the curvature is small), which reduces surface energy.

Nevertheless, some applications that demand extremely high axial uniformity, such as phase-matching for four-wave mixing across a wide bandwidth, are limited by the nanoscale fluctuations along the fiber [197]. In PBG fibers, it has been realized that capillary waves frozen at the free silica/air interfaces cause optical scattering that increases optical transmission losses [198]. In multimaterial fibers, it is expected that such instabilities will be even more significant since high surface energy may exist at the heterogeneous interfaces and the nanoscale features result in high surface curvature that increases the surface energy. We review here two such instabilities that have been studied recently in multimaterial fibers.

The wavelength of light confined in a hollow fiber core lined with a 1D cylindrical multimaterial periodic structure is determined by the refractive indices and the length of the period [199]. Guiding visible or UV light therefore necessitates reducing the thicknesses of the layers to a few tens of nanometers. An obvious question is the following: what is the thinnest such layer that may be produced stably via thermal drawing from a multimaterial preform? This question was investigated in Ref. [20] by drawing amorphous As_2Se_3 and Se thin films of various thicknesses embedded in polyethersulfone (PES) and polysulfone (PSU) polymer claddings, respectively. It was observed that the initially intact cylindrical thin film breaks up along the azimuthal direction into an array of wires that are axially continuous. The film thickness at which this breakup process occurs, which consequently determines the diameter of the resulting wires, depends on the materials combination. For As_2Se_3/PES, this breakup occurred below 10-nm film thickness, while for Se/PSU it occurred at 100 nm. The fluid dynamical origin of this striking phenomenon has been investigated from a theoretical standpoint [200], but firm conclusions have not yet been reached.

A second fluid instability occurring along the *axis* of a multimaterial fiber has been recently reported [25] [26]. In this case, a drawn multimaterial fiber consisting of a cylindrical core embedded in a cladding (Fig. 3.1a-c) is thermally treated. It was observed that heating the fiber for a sufficient period of time results in the initially intact core breaking up into a necklace of uniformly sized spheres along the fiber axis. This is a manifestation of the classical Plateau-Rayleigh capillary instability (PRI), the general tendency of fluid threads to break up into spherical droplets. As temperature increases, the viscosity of the fiber materials drop and surface tension at the heterogeneous interfaces dominates. Thermodynamically driven fluctuations arise at the interfaces, and certain fluctuation wavelengths, determined by the relative viscosity of the two materials and their surface energy, grow without bound. These wavelengths are observed as a sinusoidal modulation that develops at the core/cladding interface. The modulation depth at this instability wavelength increases until the cylindrical intact core breaks up into an array of spherical droplets. Using the classical Tomotika model [201] of the PRI, excellent agreement has been found between measurements and calculations [25] [26].

From the above we see that multimaterial fibers may be used to explore fluid dynamical problems at a wide range of length scales, and in ranges of parameters and classes of materials inaccessible to traditional micro- and nano-fluidic approaches. We anticipate that this line of research will witness considerable growth in the next few years [26].

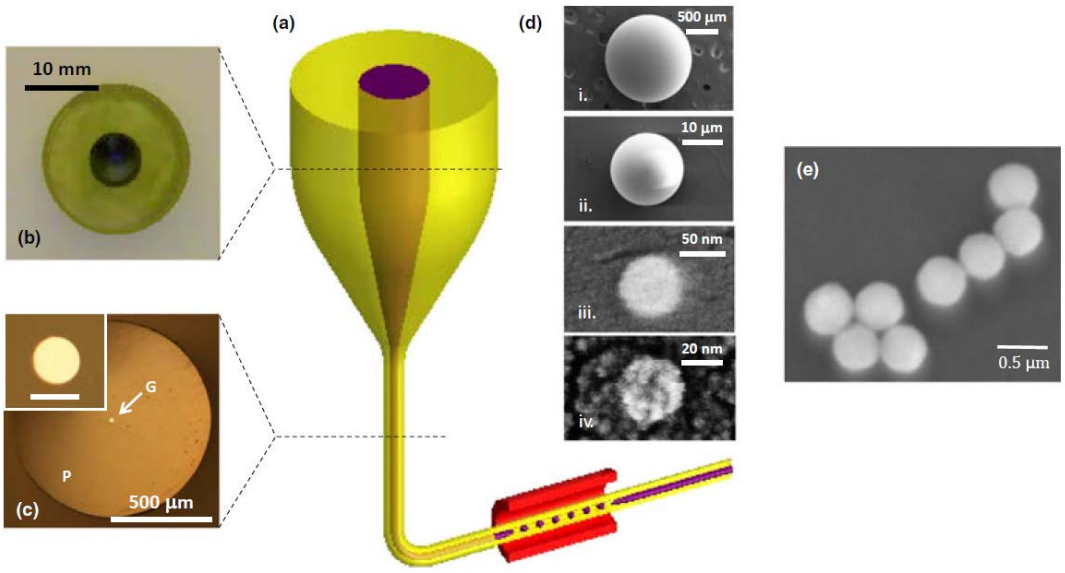

Figure 3.1 Fluid capillary instabilities in multimaterial fibers as a route to size-tunable particle fabrication. (a) A macroscopic preform is thermally drawn into a fiber. Subsequent thermal processing of the fiber induces the PRI, which results in the breakup of the intact core into spherical droplets that are frozen in situ upon cooling. (b) Photograph of a preform cross section. The core is the amorphous semiconducting chalcogenide glass As2Se3 and the cladding is the thermoplastic polymer PES. (c) Reflection optical micrograph of a fiber cross-section with 20-□m-diameter core; inset shows the core (scale bar, 20 µm). The fiber consists of an As2Se3 glass core G, encased in a PES polymer cladding P. (d) SEM images of particles with diameters: i. 1.4 mm, ii. 18 µm, iii. 62 nm, and iv. 20 nm. Adapted from Ref. [26]. (e) SEM images of Si spheres created by inducing a fluidic instability in Si-core/silica clad fibers [331].

3.3 In-fiber micron- and nano-fabrication

The ability to reduce the transverse dimensions of complex features and structures from a multimaterial preform to a fiber suggests fiber drawing as a route to nanofabrication. A multitude of potential structures may be produced in this fashion, and we will describe two here in order to give a flavor of this research direction.

3.3.1 Nanowire Fabrication by thermal fiber drawing process

Nanowires from a variety of materials have been produced using the fiber drawing process at length scales inaccessible to traditional vapor-liquid-solid processes typically used in producing nanowires. Recent work has demonstrated that amorphous and post-drawing-crystallized nanowires may be produced down to a few-nm diameter. Nanowires of amorphous Se and As_2Se_3 were produced starting from a thin film [20]. In Ref. [23], single-material and core-shell nanowires were produced, and color-control was demonstrated using a two-component nanowire in Ref. [202]. J. J. Kaufman and I investigated the lower limit of nanowire diameters stably produced by the process of thermal fiber drawing and fiber tapering. We have demonstrated that thermal fiber drawing and fiber tapering may be used to draw amorphous semiconducting nanowires to sub-5-nm diameters while maintaining axial continuity during TFD or subsequent tapering processes. Extremely long lengths of high-density, globally oriented and ordered arrays of these nanowires are combined in a single fiber. Such nanowire arrays are expected to find applications in nanosensing, nanoimaging using nanowire tips, and energy harvesting. The robustness of the nanowire bundles and their encasement in a polymer matrix scaffold further suggest important applications in live cell bioprobing.

3.3.2 Micro- and nano-particle generation

As we saw in the previous section, capillary instabilities (such as the PRI) may be controllably excited in multimaterial fibers via thermal treatment. While such fluid instabilities may be viewed as an obstacle to size reduction, they may also be viewed as an opportunity both to study fluid dynamics in new geometries, and also as a fabrication methodology to produce micro- and nanostructures, such as spherical structured nanoparticles. There is a wide range of

applications of micro- and nanoparticles, ranging from drug delivery to cosmetics that require efficient scalable pathways to producing particles over a wide range of sizes, from a variety of materials, and in a multitude of different structures. It has been recently demonstrated that an in-fiber PRI, coupled with the inherent scalability of fiber production, enables the fabrication of uniformly sized, structured spherical particles spanning an exceptionally wide range of sizes: from 2 mm down to 20 nm (Fig. 3.1d) [26]. The particles resulting from the PRI initiated by thermal treatment of the fiber are frozen *in situ* upon cooling the fiber, after which the particles are released when needed (see Fig. 3.1d). By judiciously designing the preform, the fabrication of composite, structured, spherical particles, such as core–shell particles, bi-compartmentalized 'Janus' particles, and multi-sectioned 'beach ball' particles were produced. Moreover, the process is made scalable by producing fibers with a high density of cores, which allows for an unprecedented level of parallelization [26]. Research efforts are also underway for inducing capillary breakup of Si cores in silica-clad fibers into periodic arrays of nanoscale Si spheres, which may be released from the cladding (see Fig. 3.1e) [203].

CHAPTER 4 FUTURE PROSPECTS OF MULTIMATERIAL FIBERS AND ITS APPLICATIONS

We hope to have presented an overview of the wide range of exciting ideas currently investigated in the nascent field of multimaterial fibers. The field has grown dramatically over the past decade and it is impossible to cover all the ideas being explored in this brief review. One such omission is recent work on producing multimaterial-fiber metamaterials [204] [205] [206] [207] [208]. Metamaterials are synthetic photonic structures that enable exotic optical phenomena such as cloaking [209]. By drawing arrays of metallic structures in a polymer fiber, it has been possible to demonstrate control over the electrical and magnetic resonances experienced by THz radiation transmitted through the transverse fiber cross sections. Extending this approach to optical wavelengths will require further reduction of the feature sizes in the multimaterial fibers while avoiding in-fiber fluid instabilities. Other examples include the use of gold in silica fibers for plasmonic studies and the use of soft glasses inside silica fibers for mid-infrared nonlinear applications [210] [211] [212] [213] [214] [215] [216] [217].

Further research is needed to increase the density of optical, electronic and optoelectronic devices incorporated in a multimaterial fiber. Producing fibers endowed with such functionalities in a form that may be directly woven into fabrics would be a milestone for this field, leading to a marriage of optics, electronics, and textiles. Using in-fiber capillary instabilities to produce three-dimensional macroscopic synthetic photonic structures with nanoscale control over the material distribution will enable unprecedented control over the behavior of light and sound. No doubt, further surprises lie ahead. It is safe to say that the progress in multimaterial fibers reviewed here is pointing to a renaissance in fiber fabrication that promises to continue for a long time to come.

For more details about my academia thoughts, pls Ref [218].

APPENDIX:
LIST OF PUBLICATIONS

In this Section, I list my publications during my study at CREOL, University of Central Florida by Mar. 2014. I classify these publications as following:

I have **15** published journal publications, **7** journal publications to be submitted/submitted, **17** first-author conference presentations (37 in total), **5** filed patents, **3** invited talk, and **1** book chapter.

C*itations* = **89**; h-index = **7**; *i*10-index = **5** *at* Google Scholar (update in Mar. 2014).

A. To-be-submitted/submitted Journal Articles

1. S. Shabahang, **G. Tao**, J. J Kaufman, R. S. Hoy, and A. F. Abouraddy, "Scalable fabrication of structured nano-rods and thermoreversible Venetian nano-blinds via cold drawing of multimaterial fibers," *Nature,* to be submitted, (2014).
2. **G. Tao**, et. al. "Scalable production of digitally designed spherical structured particles from multimaterial fibers," *Nature Matter.,* to be submitted, (2014).
3. **G. Tao**, et. al. "Infrared fibers: Recent developments and future prospects," ***Invited Review*** paper, *Advances in Optics and Photonics*, to be submitted (2014).
4. **G. Tao,** et. al. "Drawing robust infrared fibers from preforms produced by efficient multimaterial 'disc-to-fiber' coextrusion," *Appl. Phys. Lett.*, to be submitted (2014).
5. **G. Tao**, et. al. "The impact of temperature on the optical properties of multimaterial infrared chalcogenide glass fibers," to be submitted (2014).
6. **G. Tao**, and A. F. Abouraddy, "Development of multimaterial robust mid-infrared fibers," ***Invited Review*** paper, *Opt. Mater. Express*, to be submitted (2014).
7. H. Xu, X. Wang, Q. Nie, M. Zhu, C. Jiang, P. Zhang, S. Dai, X. Sheng, T. Xu, and **G. Tao***, "Fabrication and properties of robust multimaterial chalcogenide optical fiber based on multimaterial coextrusionm," in Chinese, *corresponding author, submitted (2014).

B. Journal Articles

1. H. Ren, **G. Tao***, A. Yang, H. Guo, G. Yang, Y. Xu, X. Wang, and Z. Yang*, "Recent developments in tellurium based chalcogenide infrared fibers (Chinese Review)," *corresponding author, *Infrared*, accepted (2014).
2. **G. Tao**, S. Shabahang, H. Ren, F. Khalizadeh-Rezaie, R. E. Peale, Z. Yang, X. Wang, and A. F. Abouraddy, "Robust multimaterial tellurium-based chalcogenide glass fibers for mid-wave and long-wave infrared transmission," *Opt. Lett.*, accepted (2014).

3. S. Shabahang, **G. Tao**, M. P. Marquez, H. Hu, T. R. Ensley, P. J. Delfyett, and A. F. Abouraddy, "Nonlinear characterization of robust multimaterial chalcogenide nanotapers for infrared supercontinuum generation," *J. Opt. Soc. Am. B*, 31 (3) 450-457 (2013).

[Highlight: B. Eggleton, Spotlight on Optics, March 2013]

4. J. J. Kaufman, R. Ottman, **G. Tao**, S. Shabahang, X. Liang, S. G. Johnson, Y. Fink, R. Chakrabarti, and A. F. Abouraddy, "In-fiber production of polymeric particles for biosensing and encapsulation," *Proc. Natl. Acad. Sci. USA*, 110, 39, 15549-15554 (2013).

5. S. Shabahang, **G. Tao**, J. J Kaufman, and A. F. Abouraddy, "Dispersion characterization of chalcogenide bulk glass, composite fibers, and robust nano-tapers," *J. Opt. Soc. Am. B*, 30 [9] 2498-2506 (2013).

6. **G. Tao**, A. M. Stolyarov, and A. F. Abouraddy, "Multimaterial fibers," *I. J. Appl. Glass Science*, 3, 349-368 (2012). ***Invited Review*** paper in the special issue, "Glass and Photonics".

[*Valuable Highlight*: Ceramic Tech Today: P. Wray, "Fiber optics of the future: Multifunctionality through multimaterials," Nov. 27, 2012;

No. 1 of the "10 most-accessed articles in *International Journal of Applied Glass Technology*" in the year of 2013 according to *the Wiley Online Library*].

7. **G. Tao,** S. Shabahang, J. J. Kaufman, and A. F. Abouraddy, "Multimaterial preform coextrusion for robust chalcogenide optical fibers and tapers", *Opt. Lett.* 37 [13] 2751-2753 (2012).

8. J. J. Kaufman, **G. Tao**, S. Shabahang, D. S. Deng, X. Liang, S. G. Johnson, Y. Fink, and A. F. Abouraddy, "Structured spheres generated by an in-fibre fluid instability," ***Nature*** 487, 463-467 (2012).

[*Valuable Highlight*: News & Views: A. Passian and T. Thundat, "Materials science: The abilities of instabilities," *Nature* 487, 440-441 (2012);

D. L. Chandler, "Dripping faucets inspire new way of creating structured particles (MIT Homepage Picture)," *MIT News Office*, 18 July, 2012; featured at Phys.org, nanowerk.com, nanotech-now.com, myscience.cc, rdmag.com (editor's pick), bioopticsworld.com, nsti.org;

M. Pollmann, "Materialwissenschaft: Wasserhahneffekt produziert vielseitige Nanopartikel," Spektrum.de (German edition of Scientific American), 18 July, 2012;

B. Abney, "UCF Nanoparticle Discovery Opens Door for Pharmaceuticals," UCF Today, 7 Aug., 2012: featured at featured at LaserFocusWorld, sciencenewsline.com, bio-medicine.org, nanowerk.com, eurekalert.org, laboratorytalk.com, humanhealthandscience.com, hematologytimes.com, sciencefreaks.co.uk, scicasts.com, www.fisher.co.uk].

9. S. Shabahang, M. P. Marquez, **G. Tao**, M. U. Piracha, D. Nguyen, P. J. Delfyett, and A. F. Abouraddy, "Octave-spanning infrared supercontinuum generation in robust chalcogenide nano-tapers using picosecond pulses," *Opt. Lett.* 37, 4639-4641 (2012).

10. X. Yu, Y. Zhou, Y. Xu, X. Wang, P. Zhang, **G. Tao**, and X. Dai, "Studies on mid-IR gain characteristics of Er^{3+}-doped chalcogenide glass photonic crystal fibers," in Chinese, *J. Optoelectronics • Laser*, (5) 915-921 (2012)
11. S. Dai, L. Lu, **G. Tao**, Y. Xu, D. Yin, W. Zhang, "Research progress of glass microspheres for optical micro-cavity (Chinese Review)," *Laser & Optoelectronics Progress,* 49, 080001 (2012).
12. J. J. Kaufman, **G. Tao**, S. Shabahang, D. S. Deng, Y. Fink, and A. F. Abouraddy, "Thermal drawing of high-density macroscopic arrays of well-ordered sub-5-nm-diameter nanowires", *Nano Lett.,* 11[11] 4768-4773 (2011).
13. **G. Tao**, H. Guo, L. Feng, M. Lu, W. Wei, and B. Peng, "Formation and properties of a novel heavy-metal chalcogenide glass doped with a high dysprosium concentration," *J. Am. Ceram. Soc.*, 92 [10] 2226-2229 (2009).
14. L. Feng, H. Guo, **G. Tao**, M. Lu, W. Wei, B. Peng, "Dy^{3+}-doped Ge-In-S-CsI chalcohalide glasses for 1.3 μm optical fiber amplifier," *J. Optoelectron. Adv. Mater.*, 11 [7] 924-928 (2009).
15. H. Guo, M. Lu, **G. Tao**, L. Feng, B. Peng, "Research progress of rare earth Ions doped chalcogenide glasses for mid-infrared luminescence (Chinese Review)," *J. Chin. Ceram. Soc.*, 37 [12] 2150-2156 (2009).

C. Invited Talks

1. **G. Tao**, S. Shabahang, H. Ren, F. Khalizadeh-Rezaie, R. E. Peale, Z. Yang, X. Wang, and A. F. Abouraddy, "Robust multimaterial tellurium-based chalcogenide glass infrared fibers," The Conference on Lasers and Electro-Optics (CLEO), San Jose, CA, June 8-13, 2014.
2. **G. Tao** and A. F. Abouraddy, "Multimaterial fibers in photonics and nanotechnology," Glass and Optical Materials Symposium, Materials Science & Technology 2014 (MS&T14), Pittsburgh, PA Oct. 12-16, 2014. (50-minute invited talk)
3. **G. Tao**, "Infrared fiber: current research progress and commercialization prospects," *Agiltron Incorporated*, Woburn, MA, July 20, 2012.

D. Conference Proceedings

1. **G. Tao**, and A. F. Abouraddy, "Multimaterial fibers: a new concept in infrared fiber optics," SPIE DSS 2014, Baltimore, MD, May 5-9 2014.
2. **G. Tao**, H. Ren, S. Shabahang, X. Wang, Z. Yang, A. F. Abouraddy, "Multimaterial rod-in-tube coextrusion for robust mid-infrared chalcogenide fibers," OPTO SPIE Photonics West, San Francisco, CA, Feb. 1 – 6 2014.
3. **G. Tao**, and A. F. Abouraddy, "Drawing robust infrared optical fibers from preforms produced by efficient multimaterial stacked coextrusion," OPTO SPIE Photonics West, San Francisco, CA, Feb. 1 – 6 2014.

4. **G. Tao**, S. Shabahang, X. Wang, and A. F. Abouraddy, "Efficient Disc-to-Fiber Multimaterial Stacked Coextrusion for Robust Infrared Optical Fibers," OSA's 97th Annual Meeting, Frontiers in Optics 2013/ Laser Science XXIX (FiO 2013/LS XXIX), Orlando, FL, October 6-10 2013. (Finalist in the 2013 Emil Wolf Outstanding Student Paper Competition).

5. S. Shabahang, **G. Tao**, M. P. Marquez, P. J. Delfyett, and A. F. Abouraddy, "Low threshold supercontinuum generation in highly nonlinear robust step-index chalcogenide nanotapers," Frontiers in Optics 2013/ Laser Science XXIX (FiO 2013/LS XXIX), Orlando, FL, October 6-10 2013.

6. S. Shabahang, **G. Tao** and, A. F. Abouraddy, "Highly nonlinear robust step-index chalcogenide nanotapers for octave-spanning supercontinuum generation," The Conference on Lasers and Electro-Optics (CLEO), San Jose, CA, June 9-14, 2013.

7. **G. Tao**, S. Shabahang, and A. F. Abouraddy, "One-step multi-material preform extrusion for robust chalcogenide glass optical fibers," OSA Advanced Photonics Congress, Specialty Optical Fibers & Applications (SOF) Topical Meeting, Colorado Springs, June 17 – 21, 2012.

8. S. Shabahang, **G. Tao**, M. Piracha, D. Nguyen, P. Delfyett, A. Abouraddy, "Octave-spanning infrared supercontinuum generation in robust chalcogenide nano-tapers," OSA Advanced Photonics Congress, Nonlinear Photonics (NP), Colorado Springs, June 17 – 21, 2012.

9. S. Shabahang, **G. Tao**, A. Abouraddy, "Optical dispersion measurements in chalcogenide glass fibers and tapers," OSA Advanced Photonics Congress, Specialty Optical Fibers & Applications (SOF) Topical Meeting, Colorado Springs, June 17 – 21, 2012.

10. J. Kaufman, **G. Tao**, S. Shabahang, A. Abouraddy, "Multimaterial fibers for generating structured nanoparticles," OSA Advanced Photonics Congress, Specialty Optical Fibers & Applications (SOF) Topical Meeting, Colorado Springs, June 17 – 21, 2012.

11. **G. Tao**, S. Shabahang, J. J. Kaufman, and A. F. Abouraddy, "One-step multi-material preform extrusion for robust chalcogenide glass optical fibers and tapers," the Conference on Lasers and Electro-Optics (CLEO), May 6-11, 2012, San Jose Convention Center, San Jose, CA, USA.

12. S. Shabahang, **G. Tao**, A. Abouraddy, "Over an octave of infrared supercontinuum generation in robust multi-material chalcogenide nano-tapers," the Conference on Lasers and Electro-Optics (CLEO), May 6-11, 2012, San Jose Convention Center, San Jose, CA, USA.

13. J. Kaufman, **G. Tao**, S. Shabahang, D. S. Deng, X. Liang, S. Johnson, Y. Fink, A. Abouraddy, "In-fiber fabrication of size-controllable structured particles," the Conference on Lasers and Electro-Optics (CLEO), May 6-11, 2012, San Jose Convention Center, San Jose, CA, USA.

14. J. J. Kaufman, **G. Tao**, and A. F. Abouraddy, "Lithographic inscription of micro-optical devices on a multi-material optical fiber tip," SPIE DSS, Orlando, FL, April 25-29 2011.

E. Refereed Conference Presentations

1. X. Wang, C. Cheng, M. Zhu, C. Jiang, F. Liao, Q. Nie, S. Dai, P. Zhang, **G. Tao** and X. Zhang, "Far-IR fiber preparation with 'High Tg" tellurium chalcohalide glass," International Symposium on Non-Oxide and New Optical Glasses (ISNOG) 2014, Aug. 24-28, 2014, Jeju, Republic of Korea

2. J. J. Kaufman, R. Ottman, **G. Tao**, S. Shabahang, , X. Liang, S. G. Johnson, Y. Fink, R. Chakrabarti, and A. F. Abouraddy, "Biosensing and micro-encapsulation in biocompatible polymeric particles produced by in-fiber fluid instabilities," MRS, 2013.
3. J. J. Kaufman, **G. Tao**, S. Shabahang, D. S. Deng, X. Liang, S. G. Johnson, Y. Fink, and A. F. Abouraddy, "Producing size-tunable structured particles via in-fiber fluid instabilities," MRS, 2013.
4. J. J. Kaufman, **G. Tao**, S. Shabahang, D. S. Deng, Y. Fink, and A. F. Abouraddy, "What is the smallest-diameter nanowire that may be thermally drawn?" Fiber Society Fall Symposium, Clemson, SC, 23 – 25 Oct., 2013.
5. **G. Tao**, S. Shabahang, A. F. Abouraddy, "Three classes of extrusion methodologies for robust multimaterial fibers," The 10th Pacific Rim Conference on Ceramic and Glass Technology (PACRIM10), including Glass & Optical Materials Division Annual Meeting (GOMD), San Diego, CA, June 2 – 7, 2013.
6. **G. Tao**, X. Wang, A. F. Abouraddy, "Robust tellurium-based chalcogenide glass fibers for far-infrared transmission produced by multimaterial Co-extrusion," The 10th Pacific Rim Conference on Ceramic and Glass Technology (PACRIM10), including Glass & Optical Materials Division Annual Meeting (GOMD), San Diego, CA, June 2 – 7, 2013.
7. **G. Tao**, Y. Xu, S. Shabahang, S. Dai, A. F. Abouraddy, "Double-piston extrusion of hybrid infrared fiber preforms," The 10th Pacific Rim Conference on Ceramic and Glass Technology (PACRIM10), including Glass & Optical Materials Division Annual Meeting (GOMD), San Diego, CA, June 2 – 7, 2013.
8. **G. Tao**, S. Shabahang, A. F. Abouraddy, "Efficient disc-to-fiber multimaterial co-extrusion for robust infrared optical fibers," The 10th Pacific Rim Conference on Ceramic and Glass Technology (PACRIM10), including Glass & Optical Materials Division Annual Meeting (GOMD), San Diego, CA, June 2 – 7, 2013.
9. **G. Tao**, J. J. Kaufman, S. Shabahang, and A. F. Abouraddy, "Scalable fabrication of digitally designed multimaterial particles enabled by in-fiber emulsification," The 10th Pacific Rim Conference on Ceramic and Glass Technology (PACRIM10), including Glass & Optical Materials Division Annual Meeting (GOMD), San Diego, CA, June 2 – 7, 2013. (Won first place prize in the GOMD Graduate Student Poster Contest).
10. J. J. Kaufman, **G. Tao**, S. Shabahang, D. S. Deng, Y. Fink, and A. F. Abouraddy, "Thermal drawing of high-density macroscopic arrays of well-ordered sub-5-nm-diameter nanowires," MRS Fall, Boston, MA, Nov. – Dec., 2012.
11. A. F. Abouraddy, J. J. Kaufman, **G. Tao**, S. Shabahang, D. S. Deng, X. Liang, S. G. Johnson, and Y. Fink, "Using in-fiber fluid instabilities for the scalable production of structured spherical particles," 65th Annual Meeting of the APS Division of Fluid Dynamics, San Diego, CA., Nov 18 – 20., 2012.
12. J. J. Kaufman, **G. Tao**, S. Shabahang, D. S. Deng, X. Liang, S. G. Johnson, Y. Fink, and A. F. Abouraddy, "Three-dimensional controlled geometric distribution of optical gain in polymer particles produced via an in-fiber fluid instability," MRS Fall, Boston, MA, Nov. – Dec., 2012.
13. J. J. Kaufman, **G. Tao**, S. Shabahang, D. S. Deng, X. Liang, S. G. Johnson, Y. Fink, and A. F. Abouraddy, "Scalable generation of structured particles through an in-fiber fluid instability," MRS Fall, Boston, MA, Nov. – Dec., 2012.

14. **G. Tao**, S. Shabahang, S. Dai, and A. F. Abouraddy, "One-step multi-material preform extrusion for robust chalcogenide glass optical fibers and tapers," XIII PNCS International Conference on the Physics of Non-Crystalline Solids (XIII PNCS), Sept. 16-20, 2012, Yichang Three Gorges, Hubei, P. R. China.
15. S. Shabahang, **G. Tao**, A. F. Abouraddy, "Optical Dispersion Control and Full-Octave Supercontinuum Generation in Robust Chalcogenide Glass Fibers and Tapers," XIII PNCS International Conference on the Physics of Non-Crystalline Solids (XIII PNCS), Sept. 16-20, 2012, Yichang Three Gorges, Hubei, P. R. China.
16. S. Danto, D. Thompson, B. Giroire, J. D. Musgraves, P. Wachtel, **G. Tao**, A. F. Abouraddy, and K. Richardson, "Synthesis of high-purity chalcogenide glasses for low-loss, high strength fibers," 18th Int. Symp. on Non-Oxide and New Optical Glasses (ISNOG), St Malo, France, July 1 – 5, 2012.
17. **G. Tao**, S. Shabahang, J. J. Kaufman, and A. F. Abouraddy, "One-step Multi-material Optical Fiber Preform Extrusion for Robust Chalcogenide Glass Optical Fibers and Tapers," The American Ceramic Society's 2012 Glass & Optical Materials Division Annual Meeting (GOMD), St. Louis, MO, May 20 – 24, 2012.
18. Z. Yang, **G. Tao**, A. F. Abouraddy, and Barry Luther-Davies, "Fabrication of chalcogenide microspheres," XIII PNCS International Conference on the Physics of Non-Crystalline Solids (XIII PNCS), Sept. 16-20, 2012, Yichang Three Gorges, Hubei, P. R. China.
19. S. Shabahang, **G. Tao**, A. Abouraddy, "Optical dispersion control and full-Octave supercontinuum generation in robust chalcogenide glass fibers and tapers," The American Ceramic Society's 2012 Glass & Optical Materials Division Annual Meeting (GOMD), St. Louis, MO, May 20 – 24, 2012.
20. J. Kaufman, S. Shabahang, **G. Tao**, and A. F. Abouraddy, "Fabrication of glassy nano-spheres via Rayleigh instabilities in multi-material fibers," TechConnect World, Nanotech 2011, Boston, MA, June 13-16 2011.

F. Other Publications on Workshops

1. **G. Tao**, S. Shabahang, H. Ren, F. Khalizadeh-Rezaie, R. E. Peale, Z. Yang, X. Wang, and A. F. Abouraddy, "Robust long-wavelength infrared tellurium-based chalcogenide glass fiber produced by multimaterial coextrusion," 2014 CREOL Affiliate Day, Advances in Optics & Photonics, CREOL, U. of Central Florida, Orlando, FL.
2. **G. Tao**, S. Shabahang, X. Wang, Y. Xu, S. Dai, and A. F. Abouraddy, "Three extrusion strategies as routes towards robust infrared multimaterial fibers," 2013 CREOL Affiliate Day, Light in Action, CREOL, U. of Central Florida, Orlando, FL.
3. **G. Tao**, S. Shabahang, J. J. Kaufman, and A. F. Abouraddy, "One-step extrusion for multimaterial structured fibers," 2012 CREOL Affiliate Day, CREOL@25 Symposium, Celebrating 25 Years of Excellence in Optics & Photonics, March 15-16, CREOL, U. of Central Florida, Orlando, FL.

4. Z. Y. Yang, B. Luther-Davies, **G. Tao**, A. F. Abouraddy, "Preparation of chalcogenide microspheres, " 11th Annual Center for Ultrahigh Bandwidth Devices for Optical Systems (CUDOS) Workshop, Shoal Bay Resort and Spa, Jan. 31-Feb. 3, 2012, New South Wales, Australia.
5. **G. Tao**, S. Shabahang, J. J. Kaufman, and A. F. Abouraddy, "Multi-material chalcogenide glass fibers for mid-infrared optics," 2011 CREOL Affiliate Day, Far IR and Terahertz Photonics, April 29, CREOL, U. of Central Florida, Orlando, FL.
6. J. J. Kaufman, S. Shabahang, **G. Tao**, and A. F. Abouraddy, "Scalable fabrication of micro- and nano-particles utilizing the Rayleigh instability in multi-material fibers," 2011 CREOL Affiliate Day, Far IR and Terahertz Photonics, April 29, CREOL, U. of Central Florida, Orlando, FL.
7. **G. Tao**, S. Shabahang, and A. F. Abouraddy, "Mid-infrared fibers for nonlinear applications," Workshop on Next-Generation Optical Fiber Technology, Cocoa Beach, FL, Oct. 18, 2010.

G. Patents

1. A. F. Abouraddy, **G. Tao**, and S. Shabahang, "Robust tellurium-based chalcogenide glass multimaterial fibers for long-wavelength infrared transmission," (filed at Feb. 2014, UCF)
2. A. F. Abouraddy, D. S. Deng, Y. Fink, S. G. Johnson, J. J. Kaufman, X. Liang, S. Shabahang, **G. Tao**," In-Fiber Particle Generation," (United States Patent Application 20130202888)
3. A. F. Abouraddy, **G. Tao**, and S. Shabahang, "Multimaterial preform extrusion for robust chalcogenide fibers and tapers," (Disclosed 05/2012, UCF). (Patents disclosures).
4. B. Peng, W. Wei, **G. Tao**, H. Guo, L. Feng, "Dysprosium-doped chalcogenide glass and preparation thereof," (Chinese Patent) (App. No. 200810202691.8).
5. B. Peng, W. Wei, **G. Tao**, L. Feng, "Novel fluorine-sulphur glass and preparation method thereof," (Chinese Patent) (App. No. 200810203052.3).

I. Books (Chapters)

1. **G. Tao**, A. F. Abouraddy, A. M. Stolyarov, and Y. Fink, "Multimaterial Fibers," Chapter One of *Lab on Fiber Technology*, A. Cusano, M. Consales, A. Crescitelli, and A. Ricciardi, Eds., (Springer, 2014).
2.

LIST OF REFERENCES

[1] G. P. Agrawal, Fiber-Optic Communication Systems, 4th Edition, *John Wiley & Sons*, Inc., Hoboken, New Jersey, 2010.

[2] R. Ramaswami, K. N. Sivarajan, and G. H. Sasaki, Optical Networks: A Practical Perspective, 3rd Edition, Morgan Kaufmann Publishers Inc., San Francisco, *California*, 2009.

[3] J. I. Peterson and G. G. Vurek, “Fiber-optic Sensors for Biomedical Applications,” Science, 13 224 123-127 (1984).

[4] A. G. Mignani and F. Baldini, "Biomedical Sensors Using Optical Fibres," *Rep. Prog. Phys.*, 59 1-28 (1996).

[5] Z. Zhou, J. He, M. Huang, J. He, and G. Chen, “Casing Pipe Damage Detection with Optical Fiber Sensors: A Case Study in Oil Well Constructions,” Advances in Civil Engineering, 2010 Article ID 638967, 9 pages, 2010.

[6] N. Mohamed, I. Jawhar, J. Al-Jaroodi, and L. Zhang, “Sensor Network Architectures for Monitoring Underwater Pipelines,” Sensors, 11 [11] 10738-10764 (2011).

[7] T. Webber, "Advances in Fiber Lasers for the Materials Processing Market," Quantum Electronics and Laser Science Conference (QELS) on Advances in High-Power Lasers and their Applications III: Processing (JTh4I), San Jose, California, USA, May 6, 2012.

[8] P. Russell, "Photonic Crystal Fibers," Science, 299 358-362 (2003).

[9] J. D. Joannopoulos, S. G. Johnson, J. N. Winn, and R. D. Meade, Photonic Crystals. Molding the Flow of Light, 2nd ed., Princeton University Press, Princeton, New Jersey, 2008.

[10] P. Russell, "Photonic Crystal Fibers: A Historical Account," IEEE LEOS Newsletters, 21 [5] 11-15 (2007).

[11] A. F. Abouraddy, M. Bayindir, G. Benoit, S. D. Hart, K. Kuriki, N. Orf, O. Shapira, F. Sorin, B. Temelkuran, and Y. Fink, "Towards Multimaterial Multifunctional Fibres that See, Hear, Sense and Communicate," Nat. Mater., 6 336-347 (2007).

[12] M. Bayindir, F. Sorin, S. Hart, O. Shapira, J. D. Joannopoulos, and Y. Fink, “Metal-Insulator-Semiconductor Optoelectronic Fibres,” Nature, 431 826-829 (2004).

[13] F. Sorin, A. F. Abouraddy, N. Orf, O. Shapira, J. Viens, J. Arnold, J. D. Joannopoulos, and Y. Fink, “Multimaterial Photodetecting Fibers: a Geometric and Structural Study,” Adv. Mat., 19 3872-3877 (2007).

[14] A. F. Abouraddy, O. Shapira, M. Bayindir, J. Arnold, F. Sorin, D. Saygin-Hinczewski, J. D. Joannopoulos, and Y. Fink, “Large-Scale Optical-Field Measurements with Geometric Fibre Constructs,” Nat. Mater., 5 532-536 (2006).

[15] M. Bayindir, A. F. Abouraddy, J. Arnold, J. D. Joannopoulos, and Y. Fink, “Thermal-Sensing Fiber Devices by Multimaterial Codrawing,” Adv. Mat., 18 845-849 (2006).

[16] M. Bayindir, O. Shapira, D. Saygin-Hinczewski, J. Viens, A. F. Abouraddy, J. D. Joannopoulos, and Y. Fink, “Integrated Fibers for Self Monitored Optical Transport,” Nat. Mater., 4 820-824 (2005).

[17] F. Sorin, O. Shapira, A. F. Abouraddy, M. Spencer, N. D. Orf, J. D. Joannopoulos, and Y. Fink, “Exploiting Collective Effects of Multiple Optoelectronic Devices Integrated in a Single Fiber,” Nano Lett., 9 2630-2635 (2009).

[18] S. Egusa, Z. Wang, N. Chocat, Z. M. Ruff, A. M. Stolyarov, D. Shemuly, F. Sorin, P. T. Rakich, J. D. Joannopoulos and Y. Fink, "Multimaterial Piezoelectric Fibres," Nat. Mater., 9 643-648 (2010).

[19] N. Chocat, G. Lestoquoy, Z. Wang, D. M. Rodgers, J. D. Joannopoulos, and Y. Fink, "Piezoelectric Fibers for Conformal Acoustics," Adv. Mat., doi: 10.1002/adma.201201355 (2012).

[20] D. S. Deng, N. D. Orf, A. F. Abouraddy, A. M. Stolyarov, J. D. Joannopoulos, H. A. Stone, and Y. Fink, “In-Fiber Semiconductor Filament Arrays,” Nano Lett., 8 4265-4269 (2008).

[21] D. S. Deng, N. D. Orf, S. Danto, A. F. Abouraddy, J. D. Joannopoulos, and Y. Fink, “Processing and Properties of Centimeter-long, In-fiber, Crystalline-Selenium Filaments,” Appl. Phys. Lett., 96 023102 (2010).

[22] M. Yaman, T. Khudiyev, E. Ozgur, M. Kanik, O. Aktas, E. O. Ozgur, H. Deniz, E. Korkut and M. Bayindir, "Arrays of Indefinitely Long Uniform Nanowires and Nanotubes," Nat. Mater., 10 494-501 (2011).

[23] J. J. Kaufman, G. Tao, S. Shabahang, D. S. Deng, Y. Fink, and A. F. Abouraddy, “Thermal Drawing of High-Density Macroscopic Arrays of Well-Ordered Sub-5-nm-Diameter Nanowires,” Nano Lett., 11 4768-4773 (2011).

[24] N. D. Orf, O. Shapira, F. Sorin, S. Danto, M. A. Baldo, J. D. Joannopoulos, and Y. Fink, “Fiber draw Synthesis,” P. Natl. Acad. Sci. USA, 108 [12] 4743-47 (2011).

[25] S. Shabahang, J. J. Kaufman, D. S. Deng, and A. F. Abouraddy, “Observation of the Plateau-Rayleigh Capillary Instability in Multi-material Optical Fibers,” Appl. Phys. Lett., 99 161909 (2011).

[26] J. J. Kaufman, G. Tao, S. Shabahang, E.-H. Banaei, D. S. Deng, X. Liang, S. G. Johnson, Y. Fink and A. F. Abouraddy, “Structured Spheres Generated by an In-Fibre Fluid Instability,” Nature, 487 463-467 (2012).

[27] M. Bayindir, A. F. Abouraddy, O. Shapira, J. Viens, D. Saygin-Hinczewski, F. Sorin, J. Arnold, J. Joannopoulos, and Y. Fink, “Kilometer-Long Ordered Nanophotonic Devices by Preform-to-Fiber Fabrication,” IEEE J. Sel. Top. Quant., 12 [6] 1202-1213 (2006).

[28] M. R. Lee, R. D. Eckert, K. Forberich, G. Dennler, C. J. Brabec, and R. A. Gaudiana, "Solar Power Wires Based on Organic Photovoltaic Materials," Science, 324 232-235 (2009).

[29] P. J. A. Sazio, A. Amezcua-Correa, C. E. Finlayson, J. R. Hayes, T. J. Scheidemantel, N. F. Baril, B. R. Jackson, D.-J. Won, F. Zhang, E. R. Margine, V. Gopalan, V. H. Crespi, and J. V. Badding, “Microstructured Optical Fibers as High-Pressure Microfluidic Reactors,” Science, 311 1583-1586 (2006).

[30] T. Li, Ed., Optical Fiber Communications: Fiber fabrication, Academic Press, Waltham, Massachusetts, 1985.

[31] H. Tokiwa, Y. Mimura, T. Nakai, O. Shinbori, "Fabrication of Long Single-Mode and Multimode Fluoride Glass Fibres by the Double-Crucible Technique," Electronics Lett., 21 [24] 1131-1132 (1985).

[32] G. Urbain, Y. Bottinga, and P. Richet, “Viscosity of Liquid Silica, Silicates and Alumino-Silicates,” Geochim. Cosmochim. Acta, 46, 1061–1072 (1982).

[33] K. Kakimoto, M. Eguchi, H. Watanabe, and T. Hibiya, "Natural and Forced Convection of Molten Silicon during Czochralski Single Crystal Growth," J Cryst. Growth 94[2] 412–420 (1989).

[34] D. Ofte, “The Viscosities of Liquid Uranium, Gold and Lead,” J. Nucl. Mater., 22 [1] 28-32 (1967).

[35] A. Napolitano and E. G. Hawkins, "Viscosity of a Standard Soda-lime-silica Glass," J. Res. NBS A Phys. Ch., 68A [5] 439-448 (1964).

[36] M. Braglia, C. Bruschi, D. Cavalli, G. Cocito, D. Guojun, J. Kraus, and S. Mosso, "Rheology of Fluoride Glasses," J. Crystal. Solid, 213-214 [12] 325-239 (1997).

[37] A. Belwalkar, W. Z. Misiolek, and J. Toulouse, "Viscosity Study of the Optical Tellurite Glass: 75TeO2-20ZnO-5Na2O,"J. Non-Crystal. Solid, 356 [1] 1354-1358 (2010).

[38] A. S. Tverjanovich, "Temperature Dependence of the Viscosity of Chalcogenide Glass-Forming Melts," Glass Phys. Chem., 29 [6] 532–536 (2003).

[39] B. Chu and K. Linliu, "Viscosity Characterization of Poly(tetrafluoroethylene) by Centrifuge Ball Viscosimetry," Macromolecules, 28 [8] 2723-2727 (1995).

[40] B. Collins, J. Shields, K. Butler, M. Seck, and T. J. Ohlemiller, "Exploring the Role of Polymer Melt Viscosity in Melt Flow and Flammability Behavior," National Inst. of Standards and Technology (BFRL), Gaithersburg, MD., ProductType: Technical report, NTIS Order Number: PB2007-105069, p 29 (2000).

[41] P. Koštál and J. Málek, "Viscosity of Selenium Melt," J. Non-Crystal. Solid, 356 [50–51] 2803-2806 (2010).

[42] V. M. Glazov, S. N. Chizhevskaya, and N. N. Glagoleva, Liquid Semiconductors, Plenum Press, New York, 1969.

[43] Y. Sato, T. Nishizuka, T. Takamizawa, T. Yamamura, and Y. Waseda, "Viscosity of Molten GaSb and InSb," Int. J. Thermophys., 23 235-243 (2002).

[44] M. F. Culpin, "The Viscosity of Liquid Indium and Liquid Tin," Proc. Phys. Soc. B, 70 [11] 1069-1078 (1957).

[45] A. Dargys and J. Kundrotas, Handbook on Physical Properties of Ge, Si, GaAs and InP, The Science and Encyclopaedia Publishing Centre, Vilnius,1994.

[46] http://www.owlnet.rice.edu/~msci301/ThermalExpansion.pdf

[47] ASM Handbook: Properties and Selection: Nonferrous Alloys and Special-Purpose Materials (ASM Handbook) VOL. 2, 10th edition, ASM International , Metals Park , OH , 1990 , 704-705 (Au) , 1154 – 1156 (Si).

[48] http://www.engineersedge.com/properties_of_metals.htm

[49] F. C. Nix, and D. MacNair, "The Thermal Expansion of Pure Metals: Copper, Gold, Aluminum, Nickel, and Iron," Phys. Rev., 60 597-605 (1941).

[50] http://www.ioffe.ru/SVA/NSM/Semicond/InSb/thermal.html

[51] D. F. Gibbons, "Thermal Expansion of Some Crystals with the Diamond Structure," Phys. Rev., 112 136-140 (1958).

[52] http://www2.dupont.com/Teflon_Industrial/en_US/tech_info/techinfo_compare.html

[53] Marvin J. Weber, Optics Handbook of Optical Materials, CRC PRESS, 2003, section 3.4 (Teflon-PTFE), section 2.4 (fused silica), section 2.2.4 (BK7) and section 2.5.1 (ZBLAN).

[54] M. Bass, E. W. Van Stryland, D. R. Williams, W. L. Wolfe, Handbook of Optics Volume II Devices, Measurements, and Properties, 2nd edition, McGraw-Hill INC. by New York, NY, 1995, p33.55 (fused Silica and ZBLAN) p7.9 (Polycarbonate).

[55] www.amorphousmaterials.com

[56] http://www.polymerprocessing.com/polymers/PC.html

[57] J. Ballato, T. Hawkins, P. Foy, R. Stolen, B. Kokuoz, M. Ellison, C. McMillen, J. Reppert, A. M. Rao, M. Daw, S. R. Sharma, R. Shori, O. Stafsudd, R. R. Rice, and D. R. Powers, "Silicon Optical Fiber," Opt. Express 16 [23]18675-18683 (2008).

[58] B. L. Scott, K. Wang, and G. Pickrell, “Fabrication of n-Type Silicon Optical Fiber,” IEEE Photon. Technol. Lett. 21 [24] 1798–1800 (2009).

[59] H. K. Tyagi, H. W. Lee, P. Uebel, M. A. Schmidt, N. Joly, M. Scharrer, and P. St. J. Russell, "Plasmon Resonances on Gold Nanowires Directly Drawn in a Step-index Fiber," Opt. Lett. 35 [15] 2573-2575 (2010).

[60] D. J. Gibson and J. A. Harrington, "Extrusion of Hollow Waveguide Preforms with a One-dimensional Photonic Bandgap Structure," J. Appl. Phys. 95 [8] 3895-3900 (2004).

[61] X. Feng, T. M. Monro, P. Petropoulos, V. Finazzi, and D. J. Richardson, "Extruded Single-mode High-index-core One-dimensional Microstructured Optical Fiber with High index-contrast for Highly Nonlinear Optical Devices," Appl. Phys. Lett. 87 [8] 081110 (2005).

[62] G. Tao, S. Shabahang, E-H Banaei, J. J. Kaufman, and A. F. Abouraddy, "Multimaterial Preform Coextrusion for Robust Chalcogenide Optical Fibers and Tapers," Opt. Lett. 37 [13] 2751-2753 (2012)

[63] M. Liao, C. Chaudhari, G. Qin, X. Yan, C. Kito, T. Suzuki, Y. Ohishi, M. Matsumoto, and T. Misumi, "Fabrication and Characterization of a Chalcogenide-tellurite Composite Microstructure Fiber with High Nonlinearity," Opt. Express 17 [24] 21608-21614 (2009).

[64] E. Snitzer and R. Tumminelli, "SiO2-clad Fibers with Selectively Volatilized Soft-glass Cores," Opt. Lett. 14 [14] 757-759 (1989).

[65] H. L. Blackmore, A Dictionary of London Gunmakers, p. 59, Phaidon - Christie's Limited, Oxford, England, 1986.

[66] E. Roeder, “Extrusion of Glass,” J. Non-Cryst. Solids, 5 [5] 377-388 (1971).

[67] E. Roeder, "Flow behaviour of glass during extrusion,” J. Non-Cryst. Solids, 7 [2] 203-220 (1972).

[68] W. Egel-Hess and E. Roeder, "Extrusion of Glass Melts-influence of Wall Friction Effects on the Die Swell Phenomenon," Glasstech. Ber., 62 [8] 279-284 (1989).

[69] D. Furniss et al., "A novel approach for drawing optical fibers from disparate core/cald. Glasses, Journal of Non-crystalline Solids 213&214, 141 (1997).

[70] D. Furniss et al., "Extrusion of gallium lanthanum sulfide glasses for fiber-optic preforms," Journal of Materials Science Letters 17, 1541 (1998).

[71] K. M. Kiang et al., "Extruded single mode non-silica glass holey optical fibers," Electronics Letters 38, 546 (2002).

[72] H. Ebendorff-Heidepriem and T. M. Monro, "Extrusion of complex preforms for microstructured optical fibers," Optics Express 15, 15086 (2007).

[73] P. Kaiser, and H. W. Astle, "Low-Loss Single-Material Fibers Made From Pure Fused Silica," AT&T Tech. J., 53 [6] 1021-1039 (1974).

[74] R. Ramsay, "Phtonic-crystal fiber characteristics benefit numerous applications," SPIE Newsroom- Sensing & Measurement (2008).

[75] B. Temelkuran, S. D. Hart, G. Benoit, J. D. Joannopoulos and Y. Fink, "Wavelength-scalable Hollow Optical Fibres with Large Photonic Bandgaps for CO_2 Laser Transmission," Nature, 420 650–653 (2002).

[76] K. Kuriki, O. Shapira, S. Hart, G. Benoit, Y. Kuriki, J. Viens, M. Bayindir, J. Joannopoulos, and Y. Fink, "Hollow Multilayer Photonic Bandgap Fibers for NIR Applications," Opt. Express, 12 [8] 1510-1517 (2004).

[77] Z. Ruff, D. Shemuly, X. Peng, O. Shapira, Z. Wang, and Y. Fink, "Polymer-composite Fibers for Transmitting High Peak Power Pulses at 1.55 microns," Opt. Express, 18 [15] 15697-15703 (2010).

[78] D. Shemuly, A. M. Stolyarov, Z. M. Ruff, L. Wei, Y. Fink, and O. Shapira, "Preparation and Transmission of Low-loss Azimuthally Polarized Pure Single Mode in Multimode Photonic Band Gap Fibers," Opt. Express 20 [6] 6029-6035 (2012).

[79] A. M. Stolyarov, A. Gumennik, W. McDaniel, O. Shapira, B. Schell, F. Sorin, K. Kuriki, G. Benoit, A. Rose, J. D. Joannopoulos, and Y. Fink, "Enhanced Chemiluminescent Detection Scheme for Trace Vapor Sensing in Pneumatically-Tuned Hollow Core Photonic Bandgap Fibers," Opt. Express, 20 [11] 12407-12415 (2012).

[80] A. M. Stolyarov, L. Wei, F. Sorin, G. Lestoquoy, J. D. Joannopoulos, and Y. Fink, "Fabrication and Characterization of Fibers with Built-in Liquid Crystal Channels and Electrodes for Transverse Incident-Light Modulation," Appl. Phys. Lett., 101 011108 (2012).

[81] A. M. Stolyarov, L. Wei, O. Shapira, F. Sorin, S. L. Chua, J. D. Joannopoulos, and Y. Fink, “Microfluidic Directional Emission Control of an Azimuthally Polarized Radial Fibre Laser,” Nature Photonics, 4 229-233 (2012)

[82] B. R. Jackson, P. J. A. Sazio and J. V. Badding, “Single-Crystal Semiconductor Wires Intetrated into Microstructured Optical Fibers,” Adv. Mat., 20 1135-1140 (2008).

[83] J. Ballato, T. Hawkins, P. Foy, C. McMillen, L. Burka, J. Reppert, R. Podila, A. Rao, R. Rice, “Binary III–V Core Semiconductor Optical Fiber,” Opt. Express, 18 [5] 4972-4979 (2009).

[84] J. R. Sparks, R. He, N. Healy, M. Krishnamurthi, A. C. Peacock, P. J. A. Sazio, V. Gopalan, and J. V. Badding, “Zinc Selenide Optical Fibers,” Adv. Mat., 23 1647-1651 (2011).

[85] D. M. Dobkin and M. K. Zuraw, Ed., Principles of Chemical Vapor Deposition, Kluwer, Dordrecht, The Netherlands, 2003.

[86] R. He, P. J. A. Sazio, A. C. Peacock, N. Healy, J. R. Sparks, M. Krishnamurthi, V. Gopalan, and J. V. Badding, "Integration of Gigahertz-bandwidth Semiconductor Devices Inside Microstructured Optical Fibres," Nat. Photonics, 6 174-179 (2012).

[87] C. C. Harb, T. K. Boyson, A. G. Kallapur, I. R. Petersen, M. E. Calzada, T. G. Spence, K. P. Kirkbride, and D. S. Moore, "Pulsed quantum cascade laser-based CRDS substance detection: real-time detection of TNT," Opt. Express 20 (14) 15489-15502 (2012)

[88] V. G. Artjushenko, P. B. Baskov, G. M. Kuz’micheva, M. D. Musina, V. V. Sakharov, T. V. Sakharova, “Structure and properties of AgCl1 − x Brx (x = 0.5–0.8) optical fibers,” Inorg. Mater. 41(2), 178-181 (2005)

[89] G. Tao, A. M. Stolyarov, and A. F. Abouraddy, “Multimaterial fibers,” I. J. Appl. Glass Science 3 (4), 349-368 (2012)

[90] F. Yu, W. J. Wadsworth, and J. C. Knight, "Low loss silica hollow core fibers for 3–4 μm spectral region," Opt. Express 20(10) 11153-11158 (2012)

[91] L. Vácha, M. Granberg, P. Marcollà, and U. Lindborg, “Manufacture of optical fibres by the double-crucible method,” J. Non-Cryst. Solids 38–39 (2), 797-802 (1980)

[92] J. F. Bei, T. M. Monro, A. Hemming, and H. Ebendorff-Heidepriem, “Reduction of scattering loss in fluoroindate glass fibers,” Opt. Mater. Express 3(9), 1285-1301 (2013)

[93] J. S. Sanghera, L. B. Shaw, I. D. Aggarwal, “Applications of chalcogenide glass optical fibers,” C.R. Chimie 5 (12), 873-883 (2002)

[94] P. Lucas, M. R. Riley, C. Boussard-Pledel, B. Bureau, “Advances in chalcogenide fiber evanescent wave biochemical sensing,” Analytical Biochemistry 351(1), 1-10 (2006)

[95] J. Troles, L. Brilland, F. Smektala, P. Houizot, F. Desevedavy, Q. Coulombier, N. Traynor, T. Chartier, T.N. Nguyen, J.L. Adam and Renversez, “ Chalcogenide microstructured fibers for infrared systems, elaboration modelization and characterization,” Fiber Integrared Opt. 28(1), 11-26 (2009)

[96] E. Lepine, Z. Yang, Y. Gueguen, J. Troles, X. Zhang, B. Bureau, C. Boussard-Pledel, J. Sangleboeuf, Pierre Lucas, “Optical microfabrication of tapers in low-loss chalcogenide fibers” J. Opt Soc Am B, 27(5), 966-971 (2010)

[97] J. Nishii, S. Morimoto, I. Inagawa, R. Iizuka, T. Yamashita and T. Yamagishi, “Recent advances and trends in chalcogenide glass fiber technology: a review,” J Non-Cryst. Solids 140 199-208 (1992)

[98] Y. Raichlin, A. Katzir, “Fiber-optic evanescent wave spectroscopy in the middle infrared,” Appl. Spectroscopy 62(2), 55A-72A (2008)

[99] R. Frerichs, “New optical glasses with good transparency in the infrared,” J. Opt. Soc. Am. 43(12), 1153–1157 (1953)

[100] N. S. Kapany and R. J. Simms, "Fiber Optics. XI. Performance in the Infrared Region," J. Opt. Soc. Am. 55(8) 963-967 (1965)

[101] S. Shibata, Y. Terunuma, T. Manabe, “Ge-P-S Chalcogenide Glass Fibers,” Jpn. J. Appl. Phys. 19, 603-605 (1980).

[102] T. Miyashita and Y. Terunuma, “Optical transmission loss of As-S glass fiber in 1.0-5.5 μm wavelenth region,” Jpn. J. Appl. Phys. 21(2) L75-L76 (1982).

[103] T. Kanamori, Y. Terunuma, S. Takahashi, and T. Miyashita, “Chalcogenide glass fibers for mid-infrared transmission,” J.of Lightwave Technology 2, 607-613 (1984).

[104] T. Katsuyama, K. Ishida, S. Satoh, and H. Matsumura, “Low loss Ge-Se chalcogenide galss optical fibers,” Appl. Phys. Lett. 45, 925-927 (1984).

[105] T. Katsuyama and H. Matsumura, “Low-loss Te-based chalcogenide galss optical fibers,” Appl. Phys. Lett. 49, 22-23 (1986).

[106] T. Katsuyama, S. Satoh, and H. Matsumura, “Scattering loss characteristics of selenide-based chalcogenide glass optical fibers,” J. App. Phys. 71, 4132-4135 (1992).

[107] T. Katsuyama and H. Matsumura, “Light transmission characteristics of telluride-based chalcogenide glass for infrared fiber application,” J. Appl. Phys. 75, 2743-2748 (1994).

[108] I. Inagawa, S. Morimoto, T. Yamashita, and I. Shirotani, “Termperature dependence of tranmission loss of chalcogenide glass fibers,” J. Appl. Phys. 36, 2229-2235 (1997).

[109] K.Itoh et.al, Drawing a chalcogenide glass fiber in a sulfur atmosphere, US Patent 5917108, 1999;

[110] H. Suto, “Chalcogenide fiber bundle for 3D spectroscopy,” Infrared Phys. Techn. 38, 93-99 (1997).

[111] J. Nishii, T. Yamashita, and T. Yamagishi, “Low-loss chalcogenide glass fiber with core-cladding structure,” Appl. Phys. Lett. 53, 553-554 (1988).

[112] J. Nishii, T. Yamashita, and T. Yamagishi, “Chalcogenide glass fiber with a core-cladding structure,” Appl. Opt. 28, 5122-5127 (1989).

[113] J. Nishii, T. Yamashita, and T. Yamagishi, “Oxide impurity absorptions in Ge-Se-Te glass fibers,” Mater. Sci. 24, 4293-4297 (1989).

[114] M. Saito, M. Takizawa, S. Sakuragi, and F. Tanei, “Infraed image guide with bundled As-S glass fibers,” Appl. Opt. 24, 2304-2308 (1985).

[115] J. Nishii, T. Yamashita, T. Yamagishi, and C. Tanaka, “Coherent infrared fiber image bundle,” Appl. Phys. Lett. 59, 2639-2641 (1991).

[116] M. Asobe, K. Suzuki, T. Kanamori, and K. Kubodera, “Nonlinear refractive index measurement in chalcogenide-glass fibers by self-phase modulation,” Appl. Phys. Lett. 60, 1153-1154 (1992).

[117] M. Asobe, H. Itoh, T. Miyazawa, and T. Kanamori, "Efficient and ultrafast all-optical switching using high delta-n, small core chalcogenide glass-fiber," Electron. Lett. 29, 1966-1968 (1993).

[118] M. Asobe, “Nonlinear optical properties of chalcogenide glass fibers and their application to all-optical switching,” Opt. fiber technol. 3, 142-148 (1997).

[119] H. Kobayashi, H. Kanbara, M. Koga, and K. Kubodera, “Third-order nonlinear optical properties of As2S3 chalcogenide glass,” J. Appl. Phys. 74, 3683-3687 (1993).

[120] S. A. Ray Hilton, Chalcogenide Glasses for Infrared Optics, McGraw-Hill, New York, 2009.

[121] M. F. Churbanov “Recent advances in preparation of high-purity chalcogenide glasses in the USSR” J. Non-Cryst. Solids 140, 324-330 (1992).

[122] M. F. Churbanov “High-purity chalcogenide glasses as materials for fiber optics” J. Non-Cryst. Sol. 184, 25-29 (1995).

[123] G. E. Snopatin, V. S. Shiryaev, V. G. Plotnichenko, E. M. Dianov and M. F. Churbanov, "High-Purity Chalcogenide Glasses for Fiber Optics," Inorganic Mat., 45, 1439-1460 (2009).

[124] M. F Churbanov, V. S. Shiryaev, I. V. Scripatchev, G. E. Snopatin, V. V. Gerasimenko, V. G. Plotnichenko, S. V. Smetanin, E. M. Dianov, I. E. Fadin and V. G. Plotnichenko, "Optical fibers based on As–S–Se glass system," J. Non-Cryst. Sol., 284, 146-152 (2001).

[125] M. F. Churbanov, I. V. Scripachev, G. E. Snopatin, V. S. Shiryaev, V. G. Plotnichenko “High-purity glasses based on arsenic chalcogenide” J. Optoelectron. Adv. Mater., 3, 341-349 (2001).

[126] M. A. Vlasov, G. G. Devyatykh, E. M. Dianov, V. G. Plotnichenko, I. V. Skripachev, V. K. Sysoev, and M. F. Churbanov, “Glassy As_2Se_3 with optical absorption of 60 dB/km,” Sov. J. Quantum Electron. [Kvantovaya Elektronika (Moscow)] 12(7), 932 (1982).

[127] V. S. Shiryaev, L. A. Ketkova, M. F. Churbanov, A. M. Potapov, J. Troles, P. Houizot, J. L. Adam and A. A. Sibirkin, "Heterophase inclusions and dissolved impurities in $Ge_{25}Sb_{10}S_{65}$ glass," J. Non-Cryst. Sol., 355, 2640-2646 (2009).

[128] V. S. Shiryaev, J. Troles, P. Houizot, L. A. Ketkova, M. F. Churbanov, J.-L. Adam, A. A. Sibirkin “Preparation of optical fibers based on Ge–Sb–S glass system” Opt. Mater. 32, 362–367 (2009).

[129] E. M. Dianov, V. G. Plotnichenko, G. G. Devyatykh, M. F. Churbanov, I. V. Scripachev,” Middle-infrared chalcogenide glass fibers with losses lower than 100 dB/Km,” Infrared Phys., 29, 303-307 (1989).

[130] A. V. Vasil'ev, G. G. Devyatykh, E. M. Dianov, A. N. Gur'yanov, A. Y. Laptev, V. G. Plotnichenko, Y. N. Pyrkov, G. E. Snopatin, I. V. Skripachev, M. F. Churbanov and V. A. Shipunov, “Two-layer chalcogenide-glass optical fibers with optical losses below 30 dB/km,” Quantum Electron. 23(2) 89 (1993).

[131] M. F. Churbanov, V. S. Shiryaev, A. I. Suchkov, A. A. Pushkin, V. V. Gerasimenko, R. M. Shaposhnikov, E. M. Dianov, V. G. Plotnichenko, V. V. Koltashev, Y. N. Pyrkov, J. Lucas, J.-L. Adam “High-Purity As–S–Se and As–Se–Te Glasses and Optical Fibers” Inorg. Mater., 43, 441–447 (2007).

[132] M. F. Churbanov, G. E. Snopatin, V. S. Shiryaev, V. G. Plotnichenko and E. M. Dianov, "Recent advances in preparation of high-purity glasses based on arsenic chalcogenides for fiber optics," J. Non-Cryst. Solid, 357, 2352-2357 (2011).

[133] I. Chiaruttini, G. Fonteneau, X.H. Zhang, J. Lucas, “Characteristics of tellurium-bromide-based glass for IR fibers optics,” J. Non-Cryst. Solid 111(1), 77-81 (1989).

[134] X. H. Zhang, H. L. Ma, G. Fonteneau, J. Lucas, “Improvement of tellurium halide glasses for IR fiber optics,” J. Non-Cryst. Solid 140, 47-51 (1992).

[135] X. H. Zhang, H. L. Ma, C. Blanchetière, J. Lucas, “New glasses based on tellurium and selenium halide for IR fiber optics,” J. Non-Cryst. Solid 146, 154-158 (1992).

[136] C. Blanchetière, K. Le Foulgoc, H. L. Ma, X. H. Zhang, J. Lucas, Tellurium halide glass fibers: preparation and applications, J. Non-Cryst. Solid 184, 200-203 (1995).

[137] X. H. Zhang, H. L. Ma, C. Blanchetière, J. Lucas, “Low loss optical fibres of the tellurium halide-based glasses, the TeX glasses,” J. Non-Cryst. Solid 161, 327-330 (1993).

[138] L. L. Neindre, F. Smektala, K. L. Foulgoc, X. H. Zhang, J. Lucas, “Tellurium halide optical fibers,” J. Non-Cryst. Solid 242(2–3) 99-103 (1998).

[139] F. Smektala, K L. Foulgoc, L. L. Neindre, C Blanchetière, X. H Zhang, J. Lucas, “TeX-glass infrared optical fibers delivering medium power from a CO_2 laser,” Opt. Mater. 13(2) 271-276 (1999).

[140] X. Zhang, H. Ma, and J. Lucas, “Applications of chalcogenide glass bulks and fibres,” J. Optoelectron. Adv. Mater.5 (5) 1327-1333 (2003).

[141] X. H. Zhang, H. Ma, J. Lucas, “Evaluation of glass fibers from the Ga–Ge–Sb–Se system for infrared applications,” Opt. Mater. 25(1) 85-89 (2004).

[142] X. H. Zhang, H. Ma, J. Lucas, Y. Guimond, S. Kodjikian, “Optical fibers and molded optics in infrared transparent glass-ceramic,” J. Non-Cryst. Solid 336(1) 49-52 (2004).

[143] V. S. Shiryaev, J.-L. Adam, X. H. Zhang, C. Boussard-Plédel, J. Lucas, M. F. Churbanov, “Infrared fibers based on Te–As–Se glass system with low optical losses, J. Non-Cryst. Solid 336(2) 113-119 (2004).

[144] V. S. Shiryaev, C. Boussard-Plédel, P. Houizot, T. Jouan, J. L. Adam, and J. Lucas, “Single-mode infrared fibers based on Te-As-Se glass system,” Mater. Sci. Eng. B 127 (2-3) 138-143 (2006).

[145] S. Maurugeon, C. Boussard-Pledel, J. Troles, A. J. Faber, P. Lucas, X. H. Zhang, J. Lucas, B. Bureau, "Telluride Glass Step Index Fiber for the far Infrared," J. Lightw. Technol. 28 (23) 3358-3363 (2010).

[146] P. Houizot, C. Boussard-Plédel, A. J. Faber, L. K. Cheng, B. Bureau, P. A. Van Nijnatten, W. L. M. Gielesen, J. Pereira do Carmo, and J. Lucas, “Infrared single mode chalcogenide glass fiber for space,” Opt. Express 15, 12529-12538 (2007).

[147] B. Bureau, S. Maurugeon, F. Charpentier, J. C. Adam, C. Boussard-Plédel, X. H. Zhang, “Chalcogenide glass fibers for infrared sensing and space optics,” Fiber Integrated Opt. 28(1) 65-80 (2009).

[148] G. Delaizir, J.-C. Sangleboeuf, E. A King, Y. Gueguen, X.-H. Zhang, C. Boussard-Pledel, B. Bureau and P. Lucas, “Influence of ageing conditions on the mechanical properties of Te–As–Se fibres,” J. Phys. D: Appl. Phys. 42 095405 (2009).

[149] J. S. Sanghera, I. D. Aggarwal, L. B. Shaw, L. E. Busse, P. Thielen, V. Nguyen, P. Pureza, S. Bayya, F. Kung, “Applications of chalcogenide glass optical fibers at NRL,” J. Optoelectron. Adv. Mater. 3(3) 1454-4164 (2001).

[150] J. S. Sanghera, I. D Aggarwal, “Development of chalcogenide glass fiber optics at NRL,” J. Non-Cryst. Solid 213–214, 63-67 (1997).

[151] J. S. Sanghera, I. D. Aggarwal, “Active and passive chalcogenide glass optical fibers for IR applications: a review,” J. Non-Cryst. Solid Volumes 256–257, 6-16 (1999).

[152] J. S. Sanghera, L. B. Shaw, L. E. Busse, V. Q. Nguyen, P. C. Pureza, B. C. Cole, B. B. Harrison, I. D. Aggarwal, R. Mossadegh, F. Kung, D. Talley, D. Roselle, R. Miklos “Development and infrared applications of chalcogenide glass optical fibers,” Fiber Integrated Opt. 19(3) 2000

[153] J. S. Sanghera, L. E. Busse, and I. D. Aggarwal, “Effect of scattering centers on the optical loss of As2S3 glass fibers in the infrared,” J. Appl. Phys. 75, 4885-4891 (1994).

[154] L. E. Busse, J. A. Moon, J. S. Sanghera, and I. D. Aggarwal, “Chalcogenide fibers enable delivery of mid-infrared laser radiation,” Laser FocusWorld, 32, 143–150 (1996).

[155] I. D. Aggarwal, L. E. Busse, L. B. Shaw, B. Cole, and J. S. Sanghera, “IR transmitting fiber and applications: High-power delivery, sources, and amplifiers,” presented at the Diode Laser Technol. Rev., Albuquerque, NM, Mar. 2–4 1998

[156] V. Q. Nguyen, J. S. Sanghera, P. C. Pureza, and I. D. Agarwal,“Effect of heating on the optical loss in the As-Se glass fiber,” J. Lightwave Tech., 12(1), 122-126 (2003).

[157] C. Florea, J. S. Sanghera, L. B. Shaw, V. Q. Nguyen, and I. D. Aggarwal, “Surface relief gratings in AsSe glass fabricated under 800-nm laser exposure,” Mater. Lett. 61, 1271-1273 (2007).

[158] Jasbinder S. Sanghera ; Ishwar D. Aggarwal ; Lynda E. Busse ; Pablo C. Pureza ; Vinh Q. Nguyen ; Robert E. Miklos ; Frederic H. Kung and Reza Mossadegh "Development of low-loss IR transmitting chalcogenide glass fibers", Proc. SPIE 2396, Biomedical Optoelectronic Instrumentation, 71 (May 1, 1995);

[159] Sanghera, J.S.; Nguyen, V.Q.; Pureza, P.C.; Kung, F.H.; Miklos, R.; Aggarwal, I.D., "Fabrication of low-loss IR-transmitting $Ge_{30}As_{10}Se_{30}Te_{30}$ glass fibers," J. Lightwave Tech., 12(5) 737-741 (1994).

[160] J. S. Sanghera, L. E. Busse, I. D. Aggarwal, "Effect of scattering centers on the optical loss of As2S3 glass fibers in the infrared," J. Appl. Phy. 75(10) 4885-4891 (1994).

[161] J. S. Sanghera, V. Q. Nguyen, P. C. Puresa, R. E. Miklos, F. H. Kung, and I. D. Aggarwal, “Fabrication of long lengths of low-loss IR transmitting $As_{40}S_{(60-X)}Se_X$ glass fibers,” J. Lightwave Tech., 14(5) 743-748 (1996).

[162] L. E. Busse, J. A. Moon, J. S. Sanghera, I. D. Aggarwal, “Chalcogenide-glass clad fiber delivers high power at mid-IR wavelengths,” Laser Focus World 32 (9) (1996).

[163] D. T. Schaafsma, L. B. Shaw, B. Cole, J. S. Sanghera, I. D. Aggarwal, "Modeling of Dy^{3+}-doped GeAsSe glass 1.3 μm optical fiber amplifiers," IEEE Photon. Technol. Lett. 10(11) 1041-1135 (1998).

[164] B. Cole, L. B. Shaw, P. C. Pureza, R. Mossadegh, J. S. Sanghera, I. D. Aggarwal, “Rare-earth doped selenide glasses and fibers for active applications in the near and mid-IR,” J. Non-Cryst. Solid 256–257, 253-259 (1999).

[165] B. Cole, L. B. Shaw, P. C. Pureza, R. Miklos, J. S. Sanghera, I. D. Aggarwal, “Core/clad selenide glass fiber doped with Pr^{3+} for active mid-IR applications,” J. Mater. Sci. 20 (5) 465-467 (2001).

[166] L. B. Shaw, B. Cole, P. A. Thielen, J. S. Sanghera, I. D. Aggarwal, "Mid-wave IR and long-wave IR laser potential of rare-earth doped chalcogenide glass fiber," IEEE J. Quantum Electro. 37(9) 1127-1137 (2001).

[167] R. S. Quimby, L. B. Shaw, J. S. Sanghera, I. D. Aggarwal, "Modeling of cascade lasing in Dy: chalcogenide glass fiber laser with efficient output at 4.5 μm," IEEE Photon. Technol. Lett. 20(2) 123-125 (2008).

[168] Z. H. Zhou, H. Nasu, T. Hashimoto, and K. Kamiya, “Non-linear optical properties and structure of Na_2S-GeS_2 glasses,” J. Non-Cryst. Solids 215, 61-67 (1997).

[168] J. S. Sanghera, L. B. Shaw, I. D. Aggarwal, "Chalcogenide glass-fiber-based Mid-IR sources and applications," IEEE J. Sel. Top. Quant. 15(1) 114-119 (2009).

[169] G. M. Camilo, "Mechanical properties of chalcogenide glasses: a review", Proc. SPIE 4940, Reliability of Optical Fiber Components, Devices, Systems, and Networks, 222 (April 25, 2003)

[170] G. G. Devyatykh, E. M. Dianov, V. G. Plotnichenko, A. A. Pushkin, Y. N. Pyrkov, I. V. Skripachev, G. E. Snopatin, M. F. Churbanov and V. S. Shiryaev, "Low-loss infrared arsenic-chalcogenide glass optical fibers", Proc. SPIE 4083, Advances in Fiber Optics, 229 (May 17, 2000)

[171] G. Tao, S. Shabahang, H. Ren, Z. Yang, X. Wang, and A. F. Abouraddy, "Robust tellurium-based chalcogenide glass multimaterial fibers for long wavelength infrared transmission," Opt. Lett., in press (2014).

[172] Y. Wang, D. Richardson, G. Brambilla, X. Feng, M. Petrovich, M. Ding, Z. Song, "Bend sensors based o periodically tapered soft glass fibers,"Proc. of SPIE Vol. 7753, 77534J (2011).

[173] M. F. Churbanov, G. E. Snopatin, V. S. Shiryaev, V. G. Plotnichenko and E. M. Dianov, "Recent advances in preparation of high-purity glasses based on arsenic chalcogenides for fiber optics," J. Non-Cryst. Sol., 357, 2352-2357 (2011).

[174] M. E. Lines "Scattering losses in optic fiber materials. II. Numerical estimates," J. Appl. Phys. 55, 4058-4063 (1984).

[175] S. Shibata, and T Manabe, "Teflon FEP-clad fluoride glass fiber," Electron. Lett., 17 [3] 128-129 (1981).

[176] T. Kanamori, Y. Terunuma, S. Takahashi, and T. Miyashita, "Chalcogenide glass fibers for Mid-Infrared transmission," J. Lightwave Technol., 2 [5] 607-613 (1984).

[177] M. Saito, M. Takizawa, S. Sakuragi, and F. Tanei, "Infrared image guide with bundled As-S glass fibers," Appl. Opt., 24 2304-2308 (1985).

[178] M. Saito and M. Takizawa, "Teflon-clad As-S glass infrared fiber with low-absorption loss," J. Appl. Phys., 59 1450-1452 (1985).

[179] J. Nishii, T. Yamashita, T. Yamagishi, C. Tanaka, and H. Sone, "Coherent infrared fiber image bundle," Appl. Phys. Lett., 59 2639-2641 (1991).

[180] H. Suto, "Chalcogenide fiber bundle for 3D spectroscopy," Infrared Phys. Techon., 38 [2], 93-99 (1997).

[181] J. S. Sanghera, V. Q. Nguyen, P. C. Pureza, R. E. Miklos, F. H. Kung, and I. D. Aggarwal, "Fabrication of long lengths of low-loss IR transmitting $As_{40}S_{(60-x)}Se_x$ glass fiber," J. Lightwave Tech., 14 [5] 743-748 (1996).

[182] C. Chaudhari, M. Liao, T. Suzuki, and Y. Ohishi, "Chalcogenide core tellurite cladding composite microstructured fiber for nonlinear applications," J. Lightwave Technol., 30 [13] 2069-2076 (2012).

[183] M. Liao, X. Yan, G. Qin, C. Chaudhari, T. Suzuki, Y. Ohishi, "Controlling the chromatic Dispersion of soft glass highly nonlinear fiber through complex microstructure," J. Non-crystal. Solids, 356 [44-49] 2613-2617 (2010).

[184] F. Luan, A. K. George, T. D. Hedley, G. J. Pearce, D. M. Bird, J. C. Knight, and P. St. J. Russell, "All-solid photonic bandgap fiber," Opt. Lett., 29 2369-2371 (2004).

[185] G. Delaizir, J.-S. Sangleboeuf, E. A. King, Y. Gueguen, X. H. Zhang, C. Boussard-Pledel, B. Bureau, and P. Lucas, "Influence of ageing conditions on the mechanical properties of Te-As-Se fibers," J. Phys. D 42, 095405 (2009).

[186] K. Itoh, K. Miura, I. Masuda, M. Iwakura, T. Yamashita, "Low-loss fluorozirco-aluminate glass fiber," J. Non-Cryst. Solids 167 (1-2) 112-116 (1994).

[187] S. D. Savage, C. A. Miller, D. Furniss, and A. B. Seddon "Extrusion of chalcogenide glass preforms and drawing to multimode optical fibers," J. Non-Cryst. Solids 354 (29) 3418–3427(2008).

[188] D. Furniss and A. B. Seddon, "Towards monomode proportioned fibreoptic preforms by extrusion," J. Non-Cryst. Solids 256-257, 232-236 (1999).

[189] T. Katsuyama and H. Matsumura, "Low-loss Te-based chalcogenide glass optical fibers," Appl. Phys. Lett. 49, 22-23 (1986).

[190] D. L. Coq, C. Boussard-Plédel, G. Fonteneau, T. Pain, B. Bureau, and J. L. Adam, "Chalcogenide double index fibers: fabrication, design, and application as a chemical sensor," Mater. Res. Bull. 38(13), 1745-1754 (2003).

[191] S. Maurugeon, C. Boussard-Plédel, J. Troles, A. J. Faber, P. Lucas, X. H. Zhang, J. Lucas, and B. Bureau, "Telluride glass step index fiber for the far Infrared," J. Lightwave Technol 28(23) 3358-3363 (2010).

[192] Z. Yang, T. Luo, S. Jiang, J. Geng, P. Lucas, "Single-mode low-loss optical fibers for long-wave infrared transmission," Opt. Lett. 35 (20) 3360-3362 (2010).

[193] X. H. Zhang, H. L. Ma, C. Blanchetière, K. L. Foulgoc, J. Lucas, J. Heuze, P. Collardelle, P. Froissard, D. Picque, and G. Corrieu, "Tellurium halide IR fibers for remote spectroscopy," Proc. SPIE 2131, 90-99 (1994).

[194]C. Blanchetiere, K. L. Foulgoc, H. L. Ma, X. H. Zhang, and J. Lucas, "Tellurium halide glass fibers: preparation and applications," J. Non-Cryst. Solids 184, 200-203 (1995).

[195] J. Ballato, C. McMillen, T. Hawkins, P. Foy, R. Stolen, R. Rice, L. Zhu, and O. Stafsudd, "Reactive molten core fabrication of glass-clad amorphous and crystalline oxide optical fibers," Opt. Mater. Express, 2 [2] 153-160 (2012).

[196] S. Morris, T. Hawkins, P. Foy, C. McMillen, J. Fan, L. Zhu, R. Stolen, R. Rice, and J. Ballato, "Reactive molten core fabrication of silicon optical fiber," Opt. Mater. Express, 1 [6] 1141-1149 (2011).

[197] S. Radic, "Parametric amplification and processing in optical fibers," Laser & Photon. Rev., 2 [6] 498-513 (2008).

[198] P. J. Roberts, F. Couny, H. Sabert, B. J. Mangan, D. P. Williams, L. Farr, M. W. Mason, A. Tomlinson, T. A. Birks, J. C. Knight, and P. St. J. Russell, "Ultimate low loss of hollow-core photonic crystal fibres," Opt. Express, 13 [1] 236-244 (2005).

[199] Y. Fink, J. N. Winn, S. Fan, C. Chen, J. Michel, J. D. Joannopoulos, and E. L. Thomas, “A dielectric omnidirectional reflector,” Science, 282 1679–1682 (1998).

[200] D. S. Deng, J.-C. Nave, X. Liang, S. G. Johnson, and Y. Fink, "Exploration of in-fiber nanostructures from capillary instability," Opt. Express 19 [17] 16273-16290 (2011).

[201] S. Tomotika, “On the instability of a cylindrical thread of a viscous liquid surrounded by another viscous fluid,” Proc. R. Soc. Lond. A 150, 322–337 (1935).

[202] T. Khudiyev, E. Ozgur, M. Yaman, and Bayindir M, "Structural coloring in large scale core-shell nanowires," Nano Lett., 11 4661-4665 (2011).

[203] A. Gumennik, L. Wei, G. Lestoquoy, A. M. Stolyarov, X. Jia, P. H. Rekemeyer, X. Liang, S. G. Johnson, A. F. Abouraddy, J. D. Joannopoulos, and Y. Fink, “Silicon-in-silica spheres via axial thermal gradient in-fibre capillary instabilities” Nat. Commun. 4 10.1038/ncomms3216 (2913).

[204] A.Tuniz, B. T. Kuhlmey, R. Lwin, A. Wang, J. Anthony, R. Leonhardt, and S. C. Fleming, "Drawn metamaterials with plasmonic response at terahertz frequencies," Appl. Phys. Lett., 96 191101 (2010).

[205] E. J. Smith, Z. Liu, Y. Mei and O. G. Schmidt, "Combined surface plasmon and classical waveguiding through metamaterial fiber design," Nano Lett., 10 1-5 (2010).

[206] A. Wang, A. Tuniz, P. G. Hunt, E. M. Pogson, R. A. Lewis, A. Bendavid, S. C. Fleming, B. T. Kuhlmey, and M. C. J. Large, "Fiber metamaterials with negative magnetic permeability in the terahertz," Opt. Mater. Express, 1 [1] 115-120 (2011).

[207] A. Tuniz, R. Lwin, A. Argyros, S. C. Fleming, E. M. Pogson, E. Constable, R. A. Lewis, and B. T. Kuhlmey, "Stacked-and-drawn metamaterials with magnetic resonances in the terahertz range," Opt. Express, 19 [17] 16480-16490 (2011).

[208] A. Tuniz, B. Pope, A. Wang, M. C. J. Large, S. Atakaramians, S-S Min, E. M. Pogson, R. A. Lewis, A. Bendavid, A. Argyros, S. C. Fleming, and B. T. Kuhlmey, "Spatial dispersion in three-dimensional drawn magnetic metamaterials," Opt. Express 20 [11] 11924-11935 (2012).

[209] R. C. McPhedran, I. V. Shadrivov, B. T. Kuhlmey and Y. S. Kivsha, “Metamaterials and metaoptics,” NPG Asia Mater., 3 100-108 (2011).

[210] N. Granzow, S. P. Stark, M. A. Schmidt, A. S. Tverjanovich, L. Wondraczek, and P. St. J. Russell, "Supercontinuum generation in chalcogenide-silica step-index fibers," Opt. Express, 19 [21] 21003-21010 (2011).

[211] H. K. Tyagi, H. W. Lee, P. Uebel, M. A. Schmidt, N. Joly, M. Scharrer, and P. St. J. Russell, "Plasmon resonances on gold nanowires directly drawn in a step-index fiber," Opt. Lett., 35 [15] 2573-2575 (2010).

[212] J. Hou, D. Bird, A. George, S. Maier, B. T. Kuhlmey, and J. C. Knight, "Metallic mode confinement in microstructured fibres," Opt. Express, 16 [9] 5983-5990 (2008).

[213] C. G. Poulton, M. A. Schmidt, G. J. Pearce, G. Kakarantzas, and P. St. J. Russell, “Numerical study of guided modes in arrays of metallic nanowires,” Opt. Lett., 32 [12] 1647-1649 (2007).

[214] M. A. Schmidt, L. N. P. Sempere, H. K. Tyagi, C. G. Poulton, and P. St. J. Russell, "Waveguiding and plasmon resonances in two-dimensional photonic lattices of gold and silver nanowires," Phys. Rev. B, 77 033417 (2008).

[215] H. W. Lee, M. A. Schmidt, H. K. Tyagi, L. N. Prill Sempere, and P. St. J. Russell, "Polarization-dependent coupling to plasmon modes on submicron gold wire in photonic crystal fiber," Appl. Phys. Lett., 93 [11] 111102 (2008).

[216] H. W. Lee, M. A. Schmidt, R. F. Russell, N. Y. Joly, H. K. Tyagi, P. Uebel, and P. St. J. Russell, "Pressure-assisted melt-filling and optical characterization of Au nano-wires in microstructured fibers," Opt. Express, 19 [13] 12180-12189 (2011).

[217] N. Granzow, P. Uebel, M. A. Schmidt, A. S. Tverjanovich, L. Wondraczek, and P. St. J. Russell, "Bandgap guidance in hybrid chalcogenide–silica photonic crystal fibers," Opt. Lett., 36 [13] 2432-2434 (2011).

[281] www.GuangmingTAO.com